UNIVERSITY OF CALIFORNIA, SAN DIEGO

Variation of the Superconductor Order Parameter in Quench-Condensed Granular Films

A dissertation submitted in partial satisfaction of the
requirements for the degree
Doctor of Philosophy

in

Physics

by

Lynne M. Merchant

Committee in charge:

Professor Robert C. Dynes, Chair
Professor Terence Hwa
Professor Huey-Lin Luo
Professor M. Brian Maple
Professor Joanna McKittrick

2000

The dissertation of Lynne M. Merchant is approved, and it is acceptable in quality and form for publication on microfilm:

University of California, San Diego

2000

This thesis is dedicated to the lives of the brave SHE fridges that died in the line of duty for my thesis. Unfortunately, they died before I attained much data. Never again will I enlist soldiers with such poor leaky arteries to fight my battles.

TABLE OF CONTENTS

LIST OF FIGURES

ACKNOWLEDGEMENTS

I acknowledge all contained in the universe. If I left anyone out, please forgive me.

VITA

1991	B. S., University of California Riverside
1992	M. S., University of California San Diego
2000	Ph. D., University of California San Diego

PUBLICATIONS

R.P. Barber, Jr., L. Merchant, A.L. Porta, and R. Dynes, Phys. Rev. B **49**, 3409 (1994).

FIELDS OF STUDY

Major Field: Experimental Condensed Matter Physics

Studies in Mathematical Physics.
Professor Marshall Rosenbluth

Studies in Theoretical Mechanics.
Professors Thomas O'Neil and Henry Abarbanel

Studies in Quantum Mechanics.
Professors Julius Kuti and Roger Dashen

Studies in Advanced Classical Electrodynamics.
Professor Herbert Levine

Studies in Equilibrium Statistical Mechanics.
Professor Daniel Dubin

Studies in Solid-State Physics.
Professor Daniel Arovas

Studies in Many-Body Theory.
Professor Daniel Arovas

Studies in Biophysics.
Professors Melvin Okamura and Jose Onuchic

ABSTRACT OF THE DISSERTATION

Variation of the Superconductor Order Parameter in Quench-Condensed Granular Films

by

Lynne M. Merchant
Doctor of Philosophy in Physics

University of California San Diego, 2000

Professor Robert C. Dynes, Chair

This thesis investigates the superconductor order parameter through variation of amplitude and phase. Quench condensed two dimensional granular Pb films probe the phase, and a proximity effect of normal metal Ag on top of a granular Pb film probes the amplitude. Experiments in this thesis show that these grains are superconducting locally even though the film may be globally insulating due to poor coupling. The granular film can be thought of as a two-dimensional array of resistively shunted Josephson junctions. Phase stiffness is explored via varying the Josephson coupling between superconducting grains. The overlap between order parameters of the grains can range from very small to very large. The larger the overlap, the stiffer the coupled grains are to resist phase fluctuations. Severe phase fluctuations can destroy superconductivity. The amplitude is related to the density of Cooper pairs and this is related to the density of states and the energy gap. The proximity effect reduces the density of Cooper pairs by allowing a larger volume for the pairs to roam in. Analogies can be made between the variation of coupling and the suppression of the order parameter amplitude in a granular Pb + Ag system and a high T_c system using the phase diagram of Emery-Kivelson theory.

Superconductivity is explored below critical temperatures of about 7 Kelvin in two dimensional quench condensed Pb films measured in a disordered granular

state, in a uniform state, in proximity to a normal metal, and in combinations of the above. Much is known about low temperature superconductors in three dimensions, but interesting questions remain in two dimensions. In two dimensions, there is a transition from an insulating state to a superconducting state that is not a sharp transition. In between lie interesting temperature dependent sheet resistance behavior. Non-insulating disordered two dimensional granular films below a bulk critical temperature exhibit a fascinating linear relation between the logarithmic sheet resistance and the temperature, $logR = logR_o + mT$, where R_o is the normal state sheet resistance above T_c. The resistive transition is wide in temperature range near the insulating side of the transition and decreases as coupling between the grains is increased. This is unusual behavior since the resistance is not a power law of temperature and not many properties vary with temperature in the numerator of the exponential. If the film is insulating, it exhibits activated behavior. With the films having a wide resistive transition, it is not clear whether the film at 0 K will exhibit insulating behavior, superconducting behavior, or in between behavior. The result depends on the coupling of grains in the disordered granular film.

Chapter 1

Introduction

This thesis explores phase fluctuations and amplitude suppresion of the superconducting order parameter near the Superconductor-Insulator transition through a series of experiments on two-dimensional quench condensed granular Pb films. The order parameter is tuned in amplitude and coupling in order to see how phase fluctuations are affected and their relation to the sheet resistance of a film below a transition temperature. Phase fluctuations are explored by weakening the coupling of superconducting regions. In a bulk superconductor, the coupling is very strong and a superconducting transition occurs rapidly below some temperature. In a two-dimensional film, the coupling is weaker, and a wider superconducting transition occurs below some temperature. Some range of temperature is required before the film is superconducting, and this transition is studied in this thesis.

Quench condensed granular Pb films provide a morphology in which each grain is superconducting, and the coupling between grains is Josephson coupling if the grains are close enough. Josephson junctions are simple systems in which coupling of superconducting order parameters can be varied. This allows the amplitude and phase of the superconducting wavefunction to be probed. For a two-dimensional film, the grains act as an array of Josephson junctions of varying coupling strengths. Quasiparticle conductance between grains and the superconductor amplitude determine this coupling strength.

Josephson junctions naturally want to lock phase, but their ability to do this depends on their strength of coupling. If there is no locked phase, there is no global superconducting state even though two superconductors comprise the Josephson junction. If there is no global superconducting state, there is a finite film resistance which varies with temperature. This film resistance is a measure of how well the grains are coupling. Thus, local and global superconductivity is explored in my thesis.

Amplitude of the superconducting order parameter is suppressed by depositing normal metal Ag on top of these Pb grains. The added volume of Ag acts to dilute the Cooper pairs, and thus the Josephson coupling amplitude can be reduced. Even though the amplitude is reduced, the grain to grain coupling is enhanced by depositions of Ag. The effect on the transition temperature below which there is local or global superconductivity is measured.

The basics of superconductivity needed to understand the experiments are given in chapter 2. Transport and tunneling measurements gather information on the energy gap Δ and the transition temperature T_c, and these important concepts are defined. The background information of electrons condensing into a superconducting state and transforming the density of states is described along with the interaction between a superconductor adjacent to another superconductor or a normal metal. Granular Pb films are composed of superconducting grains adjacent to each other, and under certain conditions, these grains couple as a resistively shunted Josephson junction. Thus the concept of Josephson junctions and their basic characteristics is important in understanding granular Pb films. Granular Pb films are also placed in proximity to a normal metal, and so the concept of a proximity effect is explained.

The morphology of a two-dimensional film can result in dramatically different transport properties. Two morphologies considered are a granular morphology and a uniform morphology. Their characteristics are explained in chapter 3 as they pass through an insulator-superconductor transition. The energy gap and transition temperature in a granular film is approximately constant as the normal

state sheet resistance increases, but the energy gap and transition temperature in a uniform film is suppressed as the normal state sheet resistance increases. The experimental methods required to form either morphology is explained in the second part of chapter 3. Similar substrates, electrical contacts, source evaporation, and measurement procedures are used in all experiments in this thesis. Due to technical difficulties, a He3/He4 dilution refrigerator was not available for all experiments, and so a simple insert stick was used that reached a base temperature of 1.7 K as opposed to a base temperature of 100 mK for the dilution refrigerator.

In chapter 4, transport and tunneling measurements are reported on quench condensed granular Pb films. Tunneling measurements on insulating Pb films surprisingly showed that the Pb grains were individually superconducting with a full energy gap. Even with disordered grains and insulating transport, superconductivity is present in grains on the order of 300 Angstroms in diameter. A discussion illustrates a possible explanation for the unique transport properties of granular Pb films. The concept of Josephson coupling is crucial in explaining the sheet resistance variation with temperature.

In chapter 5, normal metal Ag is deposited on top of an insulating quench condensed granular Pb film. The proximity effect of Ag suppresses the transition temperature as increasing amounts of Ag are deposited, but before the T_c is completely suppressed, the Ag improves coupling between the Pb grains. The improved coupling with further Ag depositions decreases the normal state sheet resistance and results in transport data nearly identical to that of an insulating granular Pb film followed by further Pb depositions. The transport can be broken down into two regions, one in which phase fluctuations are the most important and the other where amplitude suppression of the energy gap is most important. Similarities are discussed between these two regions and the two regions qualitatively described in the Emery-Kivelson theory of high T_c superconductors.

The uniform and granular morphologies are combined in chapter 6 by evaporating a base layer of electrically separate Pb grains followed by a few monolayers of Sb and then increasing depositions of either Pb or Ag. It is thought that the

morphology on top of the Sb layer is not just a uniform film, but rather a combination of a granular and uniform morphology. This leads to transport data that is a combination of granular and uniform transport. A larger range of normal state sheet resistance leads to quasi-reintrant behavior than that of granular Pb alone. Normal metal Ag deposited on top of the Sb layer surprisingly results in wide resistive transport slopes at higher normal state sheet resistance than if Pb was deposited on top of the Sb layer. Thus, phase fluctuations are suppressed faster in a Pb-Sb-Ag film than in a Pb-Sb-Pb film or a granular Pb film.

A brief summary and conclusions of the thesis are given in chapter 7. Here, the importance of superconducting order parameter wavefunction coupling is discussed. The strength of overlap is important in determining the film's susceptibility to phase fluctuations. Suggestions for further experiments are also discussed.

Chapter 2

Superconductivity, Josephson Junctions, and Proximity Effect

2.1 Superconductivity

In a superconductor, the resistance drops to zero within some hundredths of a degree. Such a rapid change in resistance was first seen by Kamerlingh Onnes [1] in 1911 when he discovered superconductivity while investigating the properties of Hg near 4 Kelvin. Although phenomenological models of superconductivity were developed in the 1940s and 1950s, it was not until 1957 that a microscopic theory was developed by Bardeen, Cooper, and Schrieffer (BCS) [2] to explain the unique properties of superconductors: the discontinuous jump in the specific heat, complete exclusion of an applied magnetic field, and zero resistance below some transition temperature T_c. BCS theory builds on the idea of Cooper [3] in 1956 that attractive pairing of electrons can lower the system energy. Lowering the system energy is a crucial requirement for any theory of superconductivity because the discontinuous jump in the specific heat suggests a second order phase transition from a disordered state into an ordered state with lower energy. The BCS theory proposes how such electrons could pair via a net attractive force, and these electron pairs are referred to as Cooper pairs.

For a Cooper pair to exist, the net force between the two electrons in a pair must be attractive. The attractive force is mediated by a virtual phonon, and if this attractive force is larger than the repulsive Coulomb force between the two electrons, the electrons form a Cooper pair. See figure 2.1. A simplified explanation of Cooper pairing is that a moving electron attracts a positive ion screened by a cloud of electrons and the ion moves enough to reveal a portion of its positive nuclear charge. A second electron moving past this ion is attracted to this revealed positive charge. The first and second electrons are coupled via the ion moving (i.e. a phonon) if this attractive electron-phonon force is larger than the repulsive electron Coulomb force. Metals like Pb and Sn have large enough electron-phonon coupling to result in Cooper pair formation and superconductivity. Metals like Au and Ag do not.

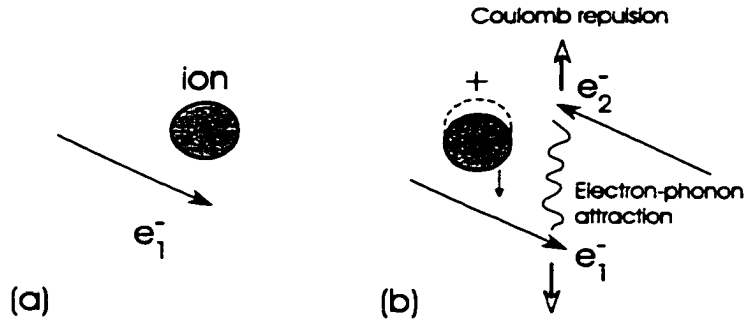

Figure 2.1: Simple explanation of a Cooper pair

(a) An electron e_1^- moves past an ion, and this motion attracts the ion to the negative charge of electron e_1^-. (b) The ion moves toward e_1^-, revealing a positive charge as it moves, and a second electron e_2^- is attracted to this positive charge. Attractive electron-phonon coupling results from this interaction and for a Cooper pair to form, this interaction must be larger than the electron-electron Coulomb repulsion.

The system energy is lowered by electron pairing, and the system energy is lowered optimally if electrons at the Fermi surface pair with opposite spin and opposite momentum. The electrons remaining coupled and satisfying this condition lie within some energy, Δ, of the Fermi energy. This energy, Δ, is referred to as

the energy gap. Since there are so many electrons available to pair, a many-body formulation is necessary to quantify the interaction. The fundamental particles, or excitations, are no longer bare electrons, but are quasiparticles: bare electrons plus a cloud of interactions with surrounding electrons and ions. A Cooper pair is then said to be composed of two quasiparticles. This Cooper pair is an extended object and is represented by some wavefunction of extension, ξ, as seen in figure 2.2.

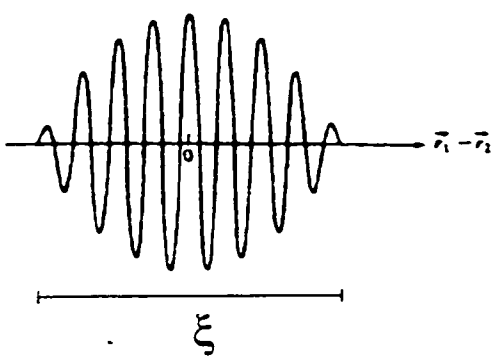

Figure 2.2: Wavefunction for a Cooper pair with a coherence length ξ

This figure was taken from VanDuzer [4]

Ginzburg and Landau in 1950 [5] provided a nice and simple way to define a superconducting state. They said that a superconducting state has some amplitude and phase, and it can be measured by a complex order parameter, $\Psi(r) = |\Psi(r)|e^{i\phi(r)}$. The amplitude measures the density of Cooper pairs at some position r and the phase measures the phase of all the Cooper pair wavefunctions at some position r. For a superconducting state to exist in some volume about r, there needs to be a finite number of Cooper pairs, and these pairs must all be locked to the same phase.

Rather than discussing superconductivity at a point r, it is better to describe

superconductivity over some volume about r. This is because a superconducting state is composed of extended Cooper pairs. A coherence length, ξ, describes the extension length of a Cooper pair over which the two quasiparticles remain bound as a pair. A coherence volume, V_{coh}, is then some volume of diameter, ξ about position r. If the coupling is strong enough between overlapping Cooper pairs, phase coherence occurs over all Cooper pairs in the volume, V_{coh}. Within this volume, there are a number of Cooper pairs, N_{coh}, and this naturally defines a Cooper pair density, N_{coh}/V_{coh}.

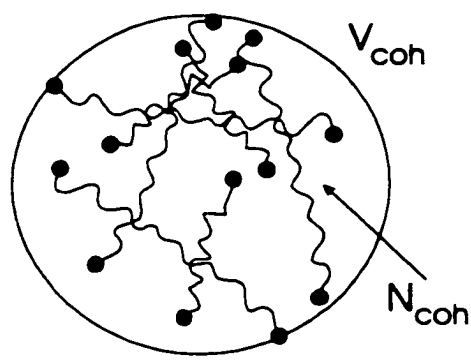

Figure 2.3: Cartoon of a coherence volume

Within a coherence volume, V_{coh}, there are a number, N_{coh}, of Cooper pairs.

Above a mean-field temperature, T_{MF}, predicted by BCS theory, quasiparticles begin to attractively pair and form Cooper pairs. A superconducting state, however, is more than just the formation of Cooper pairs. The Cooper pairs must couple to a common phase in some coherence volume below a mean-field temperature, T_{MF}. The transition of Cooper pairs to a common phase is said to be a condensation of Cooper pairs, and this state has some condensation energy lower than the disordered normal state. Each formal Cooper pair lowers the system energy by one unit of binding energy, E_b for each Cooper pair joining the collective. This condensation energy is approximately equal to the number of Cooper pairs times the binding energy. The binding energy of an isolated Cooper pair in a conventional superconductor is quite small at approximately $6\text{x}10^{-9}$ eV, but

the energy of all the Cooper pairs condensed in the system is large: $10^{-}3 - 10^{-}4$ eV. This indicates that there are approximately $10^4 - 10^5$ pairs in the system. So Cooper pairs first form from single quasiparticles, and this binding lowers the system energy. The Cooper pairs then couple with each other to form a condensate, and this further lowers the system energy. Some superconductors couple Cooper pairs into the condensate stronger than others. As more Cooper pairs join the collective, the energy needed to break a pair grows. To excite two quasiparticles out of this condensate (i.e. to break a Cooper pair) at T=0 K will take energy $2\Delta(0)$ where $\Delta(0)$ is the value of the energy gap at T=0. The condensation energy of the collective is approximately $2\Delta(0)$ times the number of Cooper pairs. Later in this chapter, a method using tunnel junctions to probe this condensation energy will be described.

Cooper pairs condense into a superconducting state within a coherence volume, V_{coh} below some temperature, T_{MF}. The energy in this volume is lowered from the normal state energy by $0.5N(0)\Delta^2 V_{coh}$ as derived in Tinkham [6]. This condensation energy is dependent on $N(0)$, Δ, and V_{coh}. If thermal energy kT is larger than this condensation energy, the coherence volume will fluctuate into a normal state and resistance results. For a stable superconducting state, the coherence volume should be resistant to thermal fluctuations, and this is achieved if $N(0)$, Δ, and/or V_{coh} are large enough. Now we have one coherence volume superconducting with some amplitude and a phase below a transition temperature T_{MF}. What about a sample size larger than this coherence volume?

To achieve long range superconductivity over the sample, coherence volumes must overlap strongly enough to lock phase among the volumes. See figure 2.4. The strength of overlap is measured by the condensation energy of the overlap between the two spheres. Such global phase coherence occurs below a film transition temperature, T_c. This distinction in transition temperatures is made because in some systems, T_{MF} and T_c do not occur at the same temperature. Anything that disturbs this binding will interrupt phase locking of these coherence volumes, and hence long range superconductivity will be disturbed. In systems such as a bulk

superconductor of Pb, T_{MF} and T_c occur nearly simultaneously. In systems such as quench condensed granular films studied in this thesis, T_{MF} and T_c do not occur simultaneously. In fact, film T_c occurs below T_{MF} in quench condensed granular films.

Phase locking is disrupted by weakening the overlap. If the coherence volumes cannot overlap sufficiently, there is not a well defined global phase. In a bulk superconductor, this is hardly an issue since the overlap is so strong. But in granular films, it is an issue. One way to weaken the overlap is to physically separate regions of coherence. This is exactly what occurs in a Josephson junction which is described later in this chapter. Here, the overlap of coherent volumes is disturbed, and this allows the phase to be probed. This overlap strength is measured by the binding energy, $E_J(T)cos(\phi_2 - \phi_1)$ where ϕ_1 and ϕ_2 are the respective phases of the overlapping coherence volumes, V_1^{coh} and V_2^{coh}. This binding energy is weaker than the condensation energy found in overlapping coherence volumes in a bulk superconductor and thus is more susceptible to phase fluctuations.

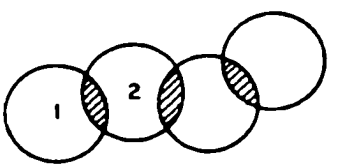

Figure 2.4: Cartoon of overlapping coherence volumes in a superconducting state. The strength of overlap is measured by the condensation energy of the overlap between the two spheres. If the overlap is strong enough to lock phase, a long range superconducting state is achieved. Figure taken from Scalapino. [7]

The condensation energy can be quantified to a condensation energy within some volume at position r using the concept of an order parameter described by Ginzburg and Landau in their theory from 1950 [5]. The superconductor order parameter describes the system macroscopically by a phenominological wavefunction with an amplitude and a phase as $\Psi(r) = |\Psi(r)|e^{i\phi(r)}$. Since the collective of Cooper pairs must have a common phase for superconductivity to exist, phase is

a very important parameter in the order parameter. The amplitude of the order parameter represents the condensation strength of supeconductivity at a position r. The order parameter can be normalized such that $\Psi^*\Psi$ represents either the density of Cooper pairs, $n_s^*(r)$, at position r or the energy gap, $\Delta(r)$. at position r. The amplitude can vary with position if there are inhomogeneities. To avoid confusion with convention in which the energy gap is actually a function of momentum. the term pair potential is used to describe the energy gap at a position r. The pair potential is a measure of the energy reduction at position r from the normal state value as Cooper pairs condense. If the system has no inhomogenieties, this value is taken as spatially constant.

Even though a superconducting state has a common phase between all Cooper pairs. Ginzburg and Landau showed that a current with zero resistance, the supercurrent, is supported by a gradient in phase. The supercurrent density is given by equation 2.1 from Tinkham [6],

$$\mathbf{J}_s = \frac{e^*}{m^*}|\Psi|^2(\hbar \bigtriangledown \phi - \frac{e^*}{c}\mathbf{A}) \tag{2.1}$$

where $\vec{A}$ is the vector potential. If the gradient is too large or the phase is discontinuous, a resistance results. Thus fluctuations in phase are important as they disturb superconductivity and can result in a resistance.

Further details of superconductivity can be found in Tinkham [6].

2.1.1 Tunnel Junctions

The quasiparticle density of states can be probed in a superconductor with a tunnel junction as was shown by Giaever [8]. This was important because the density of states allows the energy gap, Δ, to be measured. The energy gap is the measure of the energy required to break pairs. It can be measured by applying a voltage bias across a simple tunnel junction composed of a normal metal, an insulator, and a superconductor as shown in figure 2.5 and measuring the induced current. If the insulating barrier is on the order of 20 Angstroms, quasiparticles

are limited to tunneling. The tunneling current and voltage are related via the Golden rule to the quasiparticle density of states. This density of states will directly measure the energy gap as seen in figure 2.6. The absence of quasiparticle states at low voltage bias indicates the condensation of quasiparticles into Cooper pairs and a superconducting state. An energy equal to 2Δ is needed to excite quasiparticles out of the condensation, and a quasiparticle current is seen at Δ due to broken Cooper pairs.

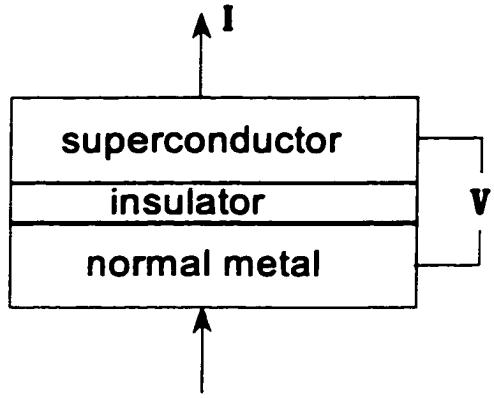

Figure 2.5: Superconductor-Insulator-Normal metal (SIN) tunnel junction

The density of quasiparticle states in a superconductor is related to the electronic density of states in the metallic state above T_c. A metal with some density of Bloch states, $N(\varepsilon)$, cooled below a transition temperature T_c will excite a certain density of states, N(E). Due to the conservation of states, the number of Bloch states created is equal to the number of Bloch states removed due to Cooper pairing. This can be expressed as $N_s(E)dE = N_n(\varepsilon)d\varepsilon$. For a superconductor, the excitation energy is $E = \sqrt{\Delta^2 + \epsilon^2}$ [4] where $\epsilon = \varepsilon - \varepsilon_F$. The energy ϵ is measured with respect to the Fermi energy ε_F. The density of electronic Bloch states $N_n(\varepsilon)$ is essentially constant near the Fermi energy, and can be approximated as $N_n(0)$. The superconducting density of states is then

$$N_s(E) = \frac{N_n(0)E}{\sqrt{E^2 - \Delta^2}} \tag{2.2}$$

In the tunnel junction model, an applied voltage V across a junction of two metals separated by an insulator raises the density of states of one metal by an amount eV. This voltage bias along with the probability of transition across the barrier, T, the density of states $N(E)$, and the fermi function $f(E)$ determine the current flow as shown in equation 2.3. The energy E is measured relative to the Fermi energy, A is a constant, and $N_r(E)$ and $N_l(E)$ refer to the density of states on the right and left side of the junction respectively.

$$I = \int_{-\infty}^{+\infty} ATN_l(E - eV)N_r(E)(f(E - eV) - f(E))dE \tag{2.3}$$

If the two metals are normal metals and the voltage bias is small, the density of states can be approximated by its value at the Fermi energy, $N(0)$ because the density of states is a weak function of E. The probability of electron transfer, T, is taken to be constant with respect to E and the current equation then reduces to equation 2.4

$$I = ATN_l(0)N_r(0) \int (f(E - eV) - f(E))dE \tag{2.4}$$

At low temperature and voltage, the integral reduces to eV which leads to an Ohmic relationship between the current and the voltage. And equation 2.4 reduces simply to

$$I = G_{NN}V \tag{2.5}$$

where G_{NN} is the normal state tunneling conductance.

If one of the metals is a normal metal and the other is a superconductor below T_c, the density of states of a superconductor in equation 2.2 must be substituted into equation 2.3 and the result is

$$I_{NS} = \frac{G_{NN}}{e} \int Re[\frac{E}{(E^2 - \Delta^2)^{1/2}}](f(E - eV) - f(E))dE \tag{2.6}$$

The conductance of the junction becomes

$$\frac{dI_{NS}}{dV} = G_{NN} \int \frac{N_S(0)}{N_N(0)}[-\frac{\partial f(E + eV)}{\partial(eV)}]dE \tag{2.7}$$

As T approaches 0 Kelvin, the equation reduces to

$$G_{NS}\,|_{T=0} = \frac{dI_{NS}}{dV}\,|_{T=0} = G_{NN}\frac{N_S(e|V|)}{N_N(0)} \tag{2.8}$$

Thus the differential conductance directly measures the superconducting density of states in the low-temperature limit. At finite temperature, some fraction of the Cooper pairs are thermally broken and there is a smearing in the dI/dV of a tunnel junction as seen in figure 2.6. The differential conductance, dI/dV, does not have a singularity at the gap edge as it does at 0 K.

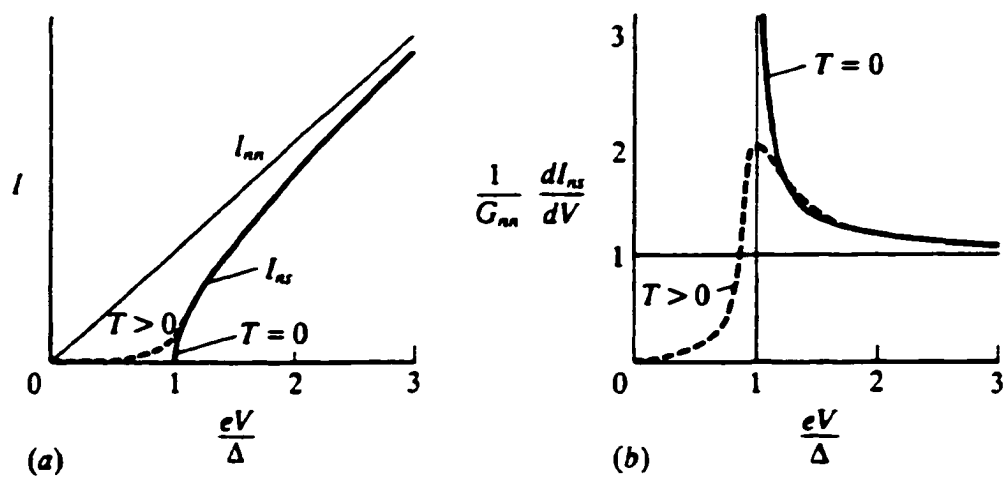

Figure 2.6: Tunneling I-V and dI/dV at T=0 and $T > 0$

(a) Tunnel I-V at T=0 and $T > 0$. (b) Differential conductance dI/dV at T=0 and $T > 0$. Both figures taken from Tinkham [6].

In the BCS theory, the Bloch density of states, $N(0)$, the strength of the electron-phonon interaction, V, and the Debye frequency of the material, ω_D are related to the energy gap Δ and the transition temperature T_c. This relation is derived in Tinkham [6]. If $N(0)V << 1$, the superconductor is said to have weak coupling between electrons and phonons. In this case, the energy gap Δ is related to $N(0)V$ by

$$\Delta = 2\hbar\omega_D e^{-1/N(0)V}, \tag{2.9}$$

and the relation between T_c and N(0)V is

$$kT_c = 1.13\hbar\omega_D e^{-1/N(0)V} \tag{2.10}$$

The value

$$\frac{2\Delta(0)}{kT_c} = 3.5 \tag{2.11}$$

is the BCS value for the assumption of weak coupling. If this value is greater than 3.5, the coupling is said to be stronger than weak coupling. Pb is a strong coupled superconductor and some corrections for the stronger coupling between electrons and phonons must be made. For Pb, the coupling value is found experimentally to be

$$\frac{2\Delta(0)}{kT_c} = 4.5 \tag{2.12}$$

2.1.2 Lifetime Broadening

Lifetime broadening is an effect seen in the density of states as a broadening of the gap edge due to the shortening of a Cooper pair lifetime. The energy broadening results from the uncertainty relation $\Delta E \Delta\tau \sim \hbar$. From the uncertainty relation, it is seen that the smaller the lifetime, the larger the energy broadening. If the energy broadening is represented by a term Γ, the lifetime broadening is on the scale of $\Gamma = \hbar/\tau$ [10]. Disorder in a material can increase electron-electron scattering, and this reduces the lifetime of a Cooper pair. The density of states is modified by replacing the energy, E, with $E - i\Gamma$ [10] where Γ is a lifetime broadening parameter.

$$N(E) = Re[\frac{E - i\Gamma}{[(E - i\Gamma)^2 - \Delta^2]^{1/2}}] \tag{2.13}$$

The lifetime of a Cooper pair can be shortened due to an interaction breaking the correlation between two electrons forming a Cooper pair. In a strong coupled

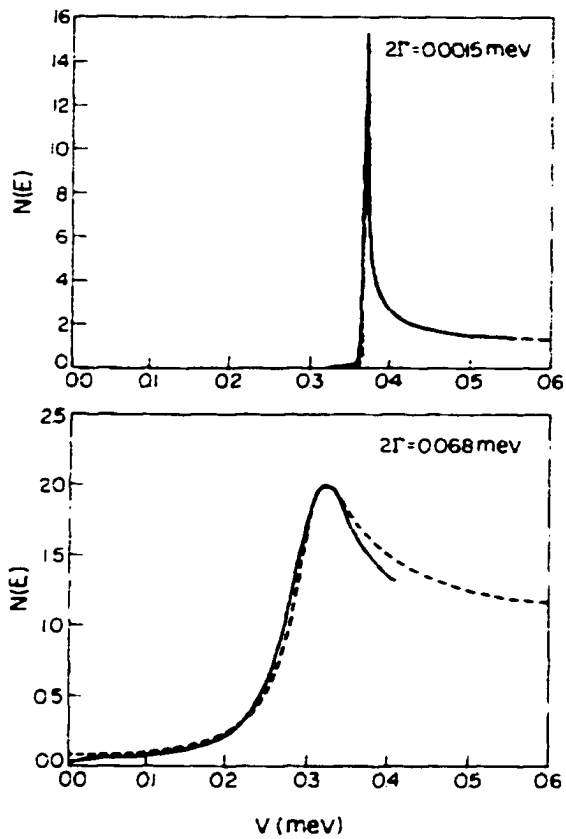

Figure 2.7: Lifetime broadening effect on density of states

Lifetime broadening of quench condensed granular Al films from data by Dynes where a higher normal state sheet resistance, larger disorder, resulted in a larger Γ and hence, a smeared gap edge in the density of states [9].

superconductor, the lifetime is shorter than that in a weak coupled superconductor due to phonon induced pair breaking. Thus, the gap edge is broadened more in a strong coupled superconductor than in a weak coupled superconductor. The effect of lifetime broadening on the density of states can be seen in figure 2.7. This data is from an experiment by Dynes [9] on granular Aluminum.

2.2 Josephson Junctions

A Josephson junction has the capability of probing both the amplitude and the phase of the superconducting order parameter. The voltage dependence probes the amplitude, the energy gap, and the supercurrent probes the phase. Probing the phase is achieved by varying the overlap between superconducting wavefunctions. If the overlap is strong enough across the barrier, both superconducting wavefunctions will reach a common phase. Until that phase is reached, a Cooper pair current is transferred to equalize the phase. In order to study this, two superconductors must be brought close enough to allow their superconductor order parameter wavefunctions to overlap so that a transfer of Cooper pairs can take place. The wavefunctions from the superconductors on the left and the right, $\Psi_{L,R} = |\Psi_{L,R}|e^{i\varphi}$, extend into the barrier and overlap as seen in figure 2.8. A junction in which two superconductors are weakly coupled by separating them with a thin barrier, a constriction, or a point contact is called a Josephson junction. This thin barrier can be a normal metal, an insulator, or a vacuum. When the two superconductors are isolated from each other, the two phases are not guaranteed to be the same across the barrier. The superconductor on the left has some phase θ_L and the superconductor on the right has some phase θ_R. Josephson [11] showed that as soon as the superconductor on the left and the superconductor on the right are brought close enough together to allow the transfer of Cooper pairs, pairs flow in a direction dependent on the phase difference $\phi = \theta_R - \theta_L$. If there was no external drawing current, a charge imbalance would stop the current when the phases equilibrate. With an external applied current, the charge transfer from

one superconductor is replenished as a supercurrent flows into the second superconductor. The supercurrent is represented by I_s, and the maximum supercurrent is represented by I_c, which is also referred to as the Josephson critical current. If the applied current is larger than I_c, a zero voltage supercurrent no longer flows and a voltage drop results. The supercurrent and the voltage induced by phase slippage are described in the Josephson equations

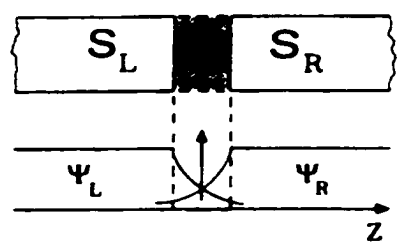

Figure 2.8: Figure of a typical Josephson junction

Overlapping superconducting wavefunctions for two superconductors separated by a barrier. Figure taken from Barone. [12]

$$I_s = I_c sin(\phi) \tag{2.14}$$

$$\frac{\partial \phi}{\partial t} = \frac{2eV}{\hbar} \tag{2.15}$$

Equation 2.15 gives the rate of phase slippage of one superconductor with respect to the other.

In a bulk superconductor, Cooper pairs condense into a state with a common phase and the overlapping of wavefunctions of common phase lowers the energy by some condensation energy. Since the overlapping wavefunctions are much more weakly coupled in the barrier of a Josephson junction, the energy is not reduced by the same amount as in a bulk superconductor. The system energy is lowered

by an amount dependent on the phase difference and tunneling resistance between the two superconductors and is referred to as the Josephson binding energy. The binding energy depends on the phase difference and is $E_J cos(\phi)$ where ϕ is the phase difference between the two superconductors. The temperature dependent Josephson binding energy E_J is

$$E_J(T) = \pi^2 N(0)^2 |M|^2 \Delta(T), \tag{2.16}$$

where $|M|^2$ is an average tunneling matrix element for electron transfer near the Fermi surface, $N(0)$ is the quasiparticle density of states at the Fermi energy, and $\Delta(T)$ is the temperature dependent energy gap. The larger the overlap of the wavefunctions, the larger E_J is. The overlap varies inversely with tunneling resistance between the superconductors. The critical current is related to the Josephson binding energy by $I_c = 2eE_J/\hbar$. If the phase difference is zero, the wavefunctions fit perfectly and the binding energy is a maximum while the supercurrent is zero. If the phase difference is $\pi/2$, the binding energy is zero, the supercurrent I_s is a maximum and equal to the critical current I_c.

A phase difference between superconductors thus induces a supercurrent to flow so that a common phase can eventually be reached. The relation between the rate of Cooper pair transfer and the phase was examined more closely by Anderson [13][14]. He first pointed out an uncertainty relation between the number of particles and the phase in a superconductor, is given by equation 2.17.

$$\Delta N \Delta\phi \sim \hbar \tag{2.17}$$

The superconducting state is described by a complex wavefunction with an amplitude and a phase. The amplitude represents the density of Cooper pairs at position r. If the charge fluctuation is represented by ΔN in any given region, the phase representing these particles is ϕ, and its uncertainty is $\Delta\phi$. Particles can move to maintain an uncertain number of particles, ΔN, at some position r. If the

transfer of particles between regions is enough to keep ΔN uncertain, the phase ϕ is fixed. This can occur within a bulk superconductor where local regions have an uncertain number of particles within them, but globally, the number of particles is fixed. The particles are free to move and so enter and leave local regions quickly. This uncertainty on a local scale is enough to keep the phase fixed while the binding energy of Cooper pairs locks the phase of local regions across the sample.

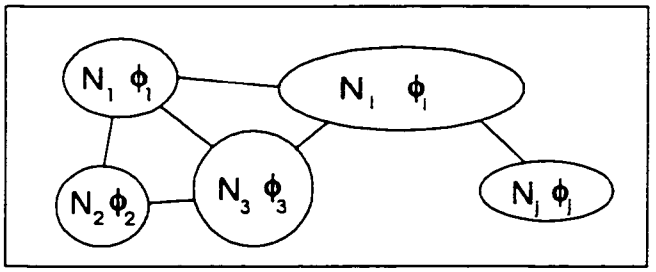

Figure 2.9: Cartoon of the uncertainty between particle number, N, and phase, ϕ

If each local region were separated from the others, it is superconducting with some total number of particles N_i and phase ϕ_i in that region. Phase coherence is maintained in each physically separated region i even though the particle number N_i is known due to the uncertainty in particle number in some smaller coherence volume. The phase of this coherence volume is then defined, and due to overlapping Cooper pairs, the phase of the entire region is defined. Phase coherence between regions i and j is only maintained if the transfer of particles is fast enough to maintain an uncertainty in $N_i - N_j$. If the uncertainty of ΔN is not large enough, the phase is not defined; the uncertainty in phase, $\Delta\phi$, is then large enough to break global phase coherence which is required for superconductivity.

For a film made up of many local regions of superconductivity, but separated such that transfer of particles is not quick enough to maintain a particle number uncertainty, each region can be treated as a bulk superconductor with a fixed phase, but the phase between regions is not fixed. This is seen in figure 2.9. Locally, within each region, the number of particles N_i varies to keep the phase ϕ_i of the region constant. But between regions i and j, the transfer of particles may not be fast enough to keep $\Delta N = N_i - N_j$ uncertain. In this case, the phase difference $\Delta\phi = \phi_i - \phi_j$ between regions i and j is uncertain. The particle flow

may be limited by the small tunneling probability between regions. The size of the supercurrent is dependent on the energy gap $\Delta(T)$ and the value of $N(0)|M|^2$ before global phase coherence is reached below a transition temperature T_c.

So far, an ideal Josephson junction has been described resulting in a supercurrent relation $I_s = I_c sin\phi$. If there is a weak link between the superconductors forming a Josephson junction, it can be described as an ideal Josephson junction shunted by a resistor and a capacitor. A resistively shunted Josephson junction allows tuning of how well Cooper pairs can transfer back and forth between the separated superconductors to decrease the uncertainty in the phase difference between them. Quasiparticle conduction gives a measure of how well a pair of qausiparticles coupled as a Cooper pair can conduct across the barrier. Until the phase difference between the superconductors is well defined and not uncertain, a supercurrent of Cooper pairs will flow trying to equalize the phase. Only when a high enough transfer rate of Cooper pairs is achieved will the uncertainty in phase be eliminated. The quasiparticle conductance limits this rate of Cooper pair transfer. The quasiparticle conductance can be limited by thermally activated hopping, a tunneling barrier, a bridge conductance, or a capacitance. If the capacitance limits how many quaisparticles can transfer to the neighboring superconductor, the current of Cooper pairs is also limited.

A resistively shunted Josephson junction can be probed by applying a dc current, I_{dc}. The system is represented by an equivalent circuit shown in figure 2.10. The Josephson junction passes a supercurrent of Cooper pairs, the resistor passes a quasiparticle current, and the capacitor passes a displacement current. The quasiparticle path is due to tunneling or energetic hopping of quasiparticles and/or a small constriction or point contact between the two superconductors. The sum of these currents is equal to the external dc current applied as shown in equation 2.18.

$$I_{dc} = C\frac{dV(t)}{dt} + GV(t) + I_c sin\phi(t) \tag{2.18}$$

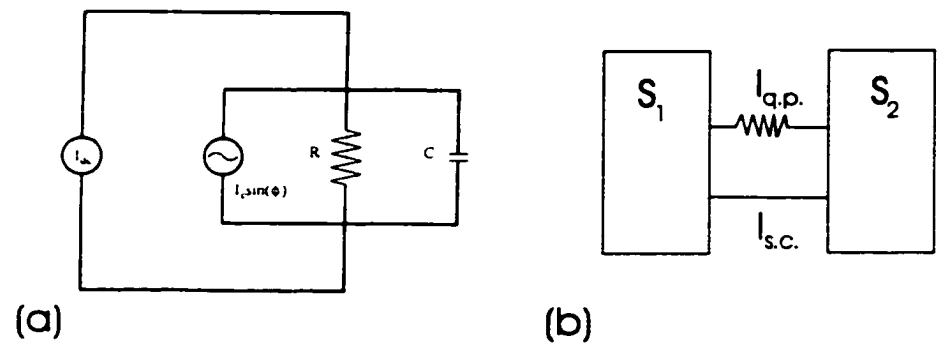

Figure 2.10: Resistively shunted Josephson junction

(a) Equivalent circuit of a resistively shunted Josephson junction with an applied dc current. (b) Quasiparticle conductance allows some quasiparticle current to flow in the normal state, and a Cooper pair conductance allows some Cooper pair current, supercurrent, to flow in the superconducting state. A supercurrent will continue to flow until the phase of S_1 and S_2 are equalized.

The voltage developed across the junction is given by the Josephson equation 2.15. This current equation is reminiscent of an equation for a damped pendulum at phase o with an external torque. With the phase difference of the Josephson junction equal to ϕ, this pendulum analogy is helpful. If the pendulum swings back and forth such that its motion never rotates the pendulum over the top, no phase slips are said to occur, and the voltage across the junction is zero. If the pendulum swings over the top, the junction is said to have undergone a 2π phase slip, and a voltage develops across the junction. The more phase slips there are, the larger the time averaged voltage across the Josephson junction. If the applied dc current is less than the critical current, there are no phase slips. If the applied dc current is larger than the critical current, phase slips occur and increase as the dc current is increased. This is described and illustrated further in figure 2.11.

Another way to represent the phase slips is with an analog to a washboard. The reason for this is that the current equation can be rewritten in a form where the motion of a particle of mass M in a bumpy potential reminiscent of a washboard represents the phase difference of the junction. This particle also lies in a viscous

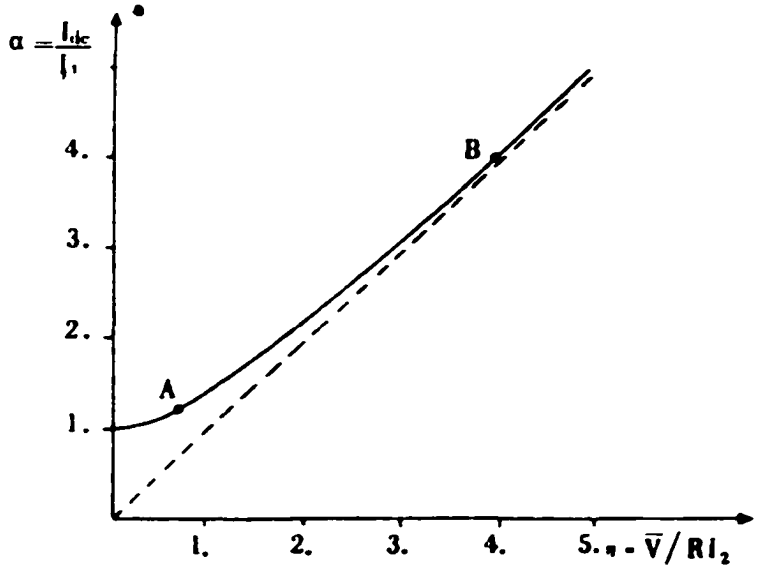

Figure 2.11: Phase slips lead to a non-zero time averaged voltage across a Josephson junction

The ratio of an applied dc current to critical current is plotted against a normalized average voltage across a resistively shunted Josephson junction. Point A corresponds to a small current ratio and hence few phase slips with a smaller average voltage than Point B which corresponds to a larger current ratio and hence many phase slips with a larger average voltage. This figure is taken from Barone [12]

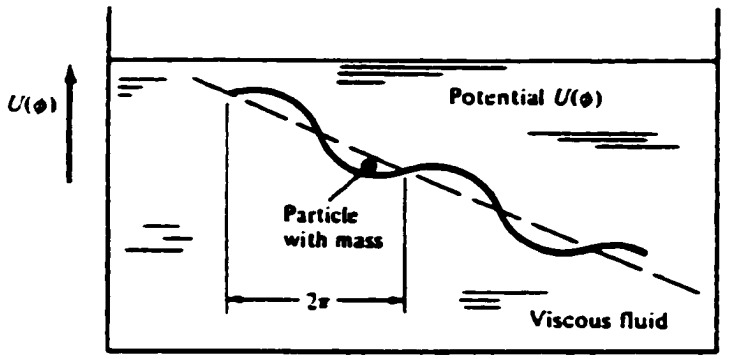

Figure 2.12: Washboard potential of a Josephson junction

The particle in the well represents the phase difference of the Josephson junction. If the particle travels to another well, a 2π phase slip occurs, and there is a corresponding voltage spike. The figure was taken from Van Duzer. [4]

fluid which represents the damping force on the pendulum. The particle in a well of the washboard is seen in figure 2.12. From Barone [12], this potential is

$$U(\phi) = -\frac{1}{2}\gamma kT(\alpha\phi + cos(\phi)). \tag{2.19}$$

where

$$\gamma = \frac{\hbar I_c(T)}{ekT} \tag{2.20}$$

and

$$\alpha = I/I_c \tag{2.21}$$

This washboard potential contains wells of depth proportional to the Josephson binding energy, $E_J(T)$. Applying a dc current is analogous to tipping the washboard and thus decreasing the well height on one side. The energy to get out of a well, $E_J cos(\phi)$, is now less than E_J. If the particle rolls to another well, this is equivalent to a 2π phase slip, and a voltage drop occurs. If the particle oscillates in the well, there is no phase slip, and so there is no time-averaged voltage drop. If thermal energy, kT, is larger than the well depth, $E_J(T)$, the particle can roll out of the well and result in a 2π phase slip.

2.3 Proximity effect

The proximity effect of a superconductor in electrical contact with a normal metal results in superconductivity existing in the normal metal due to the extension of the superconductor order parameter into the normal metal. The pair wavefunction is nonvanishing in the normal metal, and the rate at which the number of Cooper pairs decay away from the boundary depends on the diffusivity of the metal. Cooper pairs diffusing into the normal metal have a different coherence length than in the superconductor because the immediate environment in the metal is different. The density of pairs along this coherence length decays from the S-N (superconductor-normal metal) interface. The coherence length in a normal metal is given by equation 2.22,

$$\xi_n = (\frac{\hbar D_N}{2\pi k_B T})^{1/2} \tag{2.22}$$

where D_N is the diffusion coefficient of the metal. Note that this coherence length may be longer than that in the superconductor given by equation 2.23,

$$\xi_s = 0.855\frac{\sqrt{\xi_0 l_e}}{\sqrt{1-T/T_c}} \tag{2.23}$$

where ξ_0 is the coherence length in the clean limit and l_e is the elastic mean free path. For bulk Pb, $\xi_0 \sim 800$ Angstroms. In a superconducting slab of some thickness, d_s, next to a normal metal slab of thickness, d_n, (see figure 2.13) a relation can be derived for the resulting system giving an effective coupling strength, $N(0)V$. This effective $N(0)V$ can then be substituted into BCS equations for the energy gap and the transition temperature. The electrons interact via an interaction potential, $V(r)$, which is not the same in a superconductor and a normal metal. This interaction potential is positive or negative depending on the balance between Coulomb repulsion and electron-phonon attraction. In a superconductor, electron-phonon attraction is greater than Coulomb repulsion, so $V_s(r)$ is positive and is an attractive interaction. In the normal metal, if $V_n(r)$ is positive, the normal metal is a superconductor below some transition temperature. This transition

temperature may be so small, however, that it cannot be experimentally measured. If $V_n(r)$ is always negative, the interaction is repulsive.

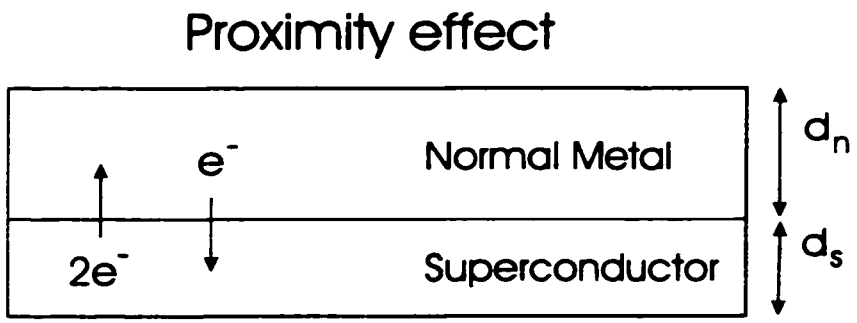

Figure 2.13: Proximity effect on electron transfer at S-N interface

Quasiparticles of charge e^- travel from the normal metal into the superconductor. Cooper pairs of charge $2e^-$ travel from the superconductor into the normal metal.

If the thicknesses d_n and d_s are much smaller than their respective coherence lengths ξ_n and ξ_s, the system is said to be in the Cooper limit. In this limit, Cooper pairs can extend throughout the normal metal with the density of pairs larger near the S-N interface. Cooper [15] made a simplifying assumption that the interaction potential between electrons was positive and equal to V in the superconductor slab, but that V was equal to zero in the normal metal slab. Over the volume of the superconducting slab, there is some average value $[N(0)V]_s$. Over the entire volume of the superconducting and normal metal slabs, there is some average value $[N(0)V]_{s+n}$. Since the interaction is now averaged over a larger volume that includes both the superconductor and the normal metal, $[N(0)V]_{s+n}$ will be less than $[N(0V]_s$; the electron-phonon interaction only takes place over part of the volume, but the electron normalization volume is increased. The Cooper pairs can flow over a larger volume, but the interaction potential only occurs in part of the volume. The relation for this new value of $[N(0)V]_{s+n}$ is simply

$$[N(0)V]_{s+n} = \frac{d_s}{d_s + d_n}[N(0)V]_s \tag{2.24}$$

According to deGennes [16], the interaction potential in the normal metal must be taken into account. Where before, only $N(0)$ and V only referred to the superconductor, in the deGennes model, there is a density of states, $N_{s,n}(0)$, and interaction potential, $V_{s,n}$, respectively for the superconductor and the normal metal. If this is done, a new value of $[N(0)V]_{av}$ is given by equation 2.25.

$$[N(0)V]_{av} = \frac{V_n(N_n(0))^2 d_n + V_s(N_s(0))^2 d_s}{N_n(0)d_n + N_s(0)d_s} \tag{2.25}$$

A modification of N(0)V affects the energy gap through the gap equation $\Delta = 2\hbar\omega_D e^{-1/N(0)V}$ where any small changes in the exponent result in large changes in the energy gap. The transition temperature is affected through $kT_c = 1.13\hbar\omega_D e^{-1/N(0)V}$.

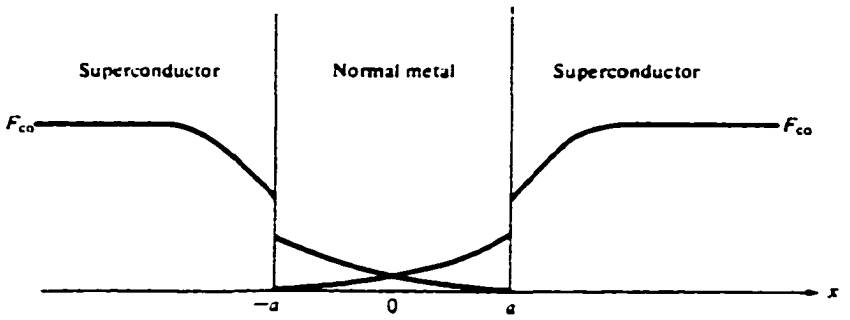

Figure 2.14: Decay of superconductor wavefunction in a normal metal

The probability of finding a Cooper pair at position r, F(r), is plotted for a superconductor next to a normal metal. The probability is discontinuos across the boundary, but is finite in the normal metal. This figure was taken from VanDuzer [4]

The energy gap for a superconductor measures half the energy needed to remove a Cooper pair from the condensate. The energy needed to remove a Cooper pair depends on the density of Cooper pairs at the position where the pair is removed: the denser the pairs, the larger the condensation energy. With an inhomogeneous

system of a superconductor slab in proximity to a normal metal slab, Cooper pairs and quasiparticles can flow across the S-N interface. The density of Cooper pairs thus varies across this interface as seen in figure 2.14 where $F(r)$ is the probability of finding a Cooper pair at position r. This figure is for thicknesses greater than the Cooper limit, $\xi <$ slab thickness. Thus the superconducting wavefunction rapidly decreases in the normal metal. In the Cooper limit, the superconducting wavefunction does not decrease so rapidly.

Since the interaction potential V also varies with position, the pair potential $\Delta(r) = V(r)F(r)$ measures the condensation energy with position. The density of states measured by tunneling gives information about the energy gap over all momentum states. At some position r, this energy gap over all momentum states varies. So the tunneling measurement can only give information about the weighted-average of the energy gap over position. The larger the volume of normal metal provided for the Cooper pairs to roam in, the lower the average density of Cooper pairs at some position r, and the lower the average value of the energy gap. Thus the order parameter amplitude decreases as the same number of Cooper pairs roam a larger volume. This effect results in a reduced Δ and T_c.

Chapter 3

Morphology and experimental methods

3.1 Morphology and the S-I transition

Disorder is inherent in two-dimensional films [17] and disturbs the superconducting order parameter below T_{MF}. Two-dimensional films are usually either granular in which the film is broken up into grains exposing spots of the substrate or uniform in which the film covers the substrate completely and can be a very thin film. In a granular morphology, phase locking of the order parameter is disturbed. In a uniform morphology, amplitude of the order parameter is disturbed. This is perfect for probing the effects of phase fluctuations and order parameter amplitude suppression on the global superconductivity of a film. Two-dimensional films naturally lend themselves to study fluctuations since they are so susceptible to fluctuations. A three-dimensional film is much more robust against fluctuations.

It is the varying Josephson coupling strengths in a two-dimensional granular film that make it so interesting. The poor quasiparticle conduction in a two-dimensional film allows Josephson coupling to be varied over a large range of sheet resistance. With just a few Angstroms of Pb deposited, the coupling can be drastically affected in a two-dimensional film. To study amplitude suppression, a

three-dimensional film of Pb would need a normal metal evaporated on top in order to suppress the order parameter amplitude. A uniform morphology inherently does this by virtue of how thin and disordered it is.

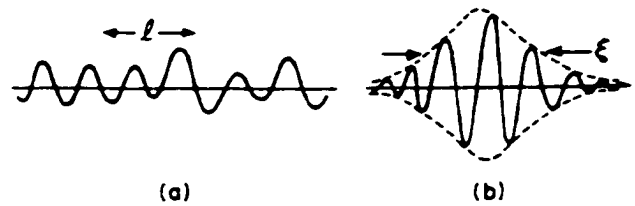

Figure 3.1: Extended and localized wavefunctions

(a) Extended state with a mean free path of l. (b) Localized state with a localization length of ξ. Figure taken from Lee. [18]

Anything that can affect the coherence properties of a superconducting state is very important. Localization is an important concept because it is a limiting length scale and affects the coherence length. Localization does exactly as the name implies and localizes a wavefunction to a wavepacket exponentially decaying at the ends. This wavefunction can refer to either an electron or to a superconducting order parameter. In the case of single electrons, overlap of localized wavefunctions can lead to an extended state and metallic behavior. In the case of superconducting order parameters, overlap can determine long range superconductivity. In less than three dimensions, the question of overlap and conduction becomes more important as even weak disorder can effect large changes. What effect this will have on a superconducting state becomes important as the dimension is reduced. Dimension is defined by the relative size of the coherence length and film dimension. If the coherence length is larger than the film thickness, the film is two-dimensional. One-dimensional wires are not discussed in this thesis.

Long range superconductivity requires overlap of superconducting wavefunctions. The overlap must be strong enough to couple all wavefunctions to a common phase. This is not a requirement for a metallic state. A metallic state requires

extended states, but a superconducting state requires an extended state with a well defined phase. If the disorder disrupts the number of Cooper pairs in the superconducting state or the ability of the wavefunctions to overlap, then superconductivity is affected by disorder. If disorder suppresses the coherence length, a smaller coherence volume reduces overlap. A reduced overlap may not be strong enough to maintain a common phase. Temperature also affects the coherence length. Lowering the temperature will increase the effective coherence length and allows larger overlap.

The superconductor-Insulator (S-I) transition is defined in terms of extended electron wavefunctions in the superconducting state and localized electron wavefunctions in the insulating state. Experiments and theories have proposed that the superconducting state is intimately connected with the normal state [19]. Electrical conduction in the normal state results if there is a finite density of Bloch states across the sample. The density of Bloch states at the Fermi energy, $N(0)$, can affect how many Cooper pairs can form. The normal state can also affect superconductivity by limiting overlap below T_c.

A superconductor-insulator transition is a transition from long range phase coherent superconductivity to an insulating state composed of localized wavefunctions. In the superconducting state, the wavefunction refers to a coordinated condensation of pairs rather than the wavefunction of a single electron. This superconducting wavefunction is represented as an order parameter with an amplitude and a phase. $\Psi(r) = \Delta^{1/2}(r)e^{i\phi}$. Superconductivity is destroyed if the amplitude is suppressed and/or the phase fluctuates. Thus the S-I transition is interesting in that there is an opportunity to probe the formation of Cooper pairs and their coupling in relation to the quasiparticle sheet resistance.

The long-range superconducting state is broken up by fluctuations in amplitude and/or phase of the global wavefunction across the sample length as disorder increases. This is seen in both the uniform and granular morphology, but manifests itself in different ways. (((Explain more on uniform film and amplitude fluctuations.))) Many experiments have probed the characteristics of granular films

composed of superconducting metals such as Al, Pb, and Sn [20][21] [22] [23]. They find a gradual transition from a superconducting state with global phase coherence to a state coupling wavefunctions of varying phase to a strongly localized state in which wavefunctions are not coupled with each other across the sample length. The insulating state may contain completely randomized localized wavefunctions as in the uniform morphology or it may contain phase coherent wavefunctions localized within some region smaller than the sample length as in the granular morphology.

3.1.1 Uniform morphology

A uniform morphology is formed by evaporating a material on top of a few monolayers of Sb or Ge as shown in figure 3.2. This morphology occurs because Ge/Sb has dangling bonds that bind the Pb atoms as they are deposited and decreases their lateral mobility. The thin film is initially insulating but electrical continuity is achieved at about 5-10 Angstroms of Pb. At the metal-insulator transition of thin uniform normal metals, the Bloch density of states N(0) goes to zero. This has important consequences for the S-I transition of a uniform film. Increased Coulomb interactions reduce N(0) and hence the number of states available to form Cooper pairs. As more Pb is deposited, superconductivity appears with a T_c suppressed far below the bulk value. The T_c is suppressed because the disorder results in enhanced interactions between electrons which hinders the net attractive force needed to form Cooper pairs. Even though the net attractive force is hindered by enhanced Coulomb interactions, Dynes [24] found that the value of $2\Delta/kT_c$ remained constant at the strong coupled value of 4.5 right up to the S-I transition in ultrathin films of quench condensed Bi. Thus as T_c approached zero. Δ approached zero proportionately to maintain the strong coupled value of $2\Delta/kT_c$.

The amplitude of the order parameter decreases as the S-I transition is approached from the superconducting side, and a small amplitude is susceptible to fluctuations which can destroy superconductivity. Thus, amplitude fluctuations

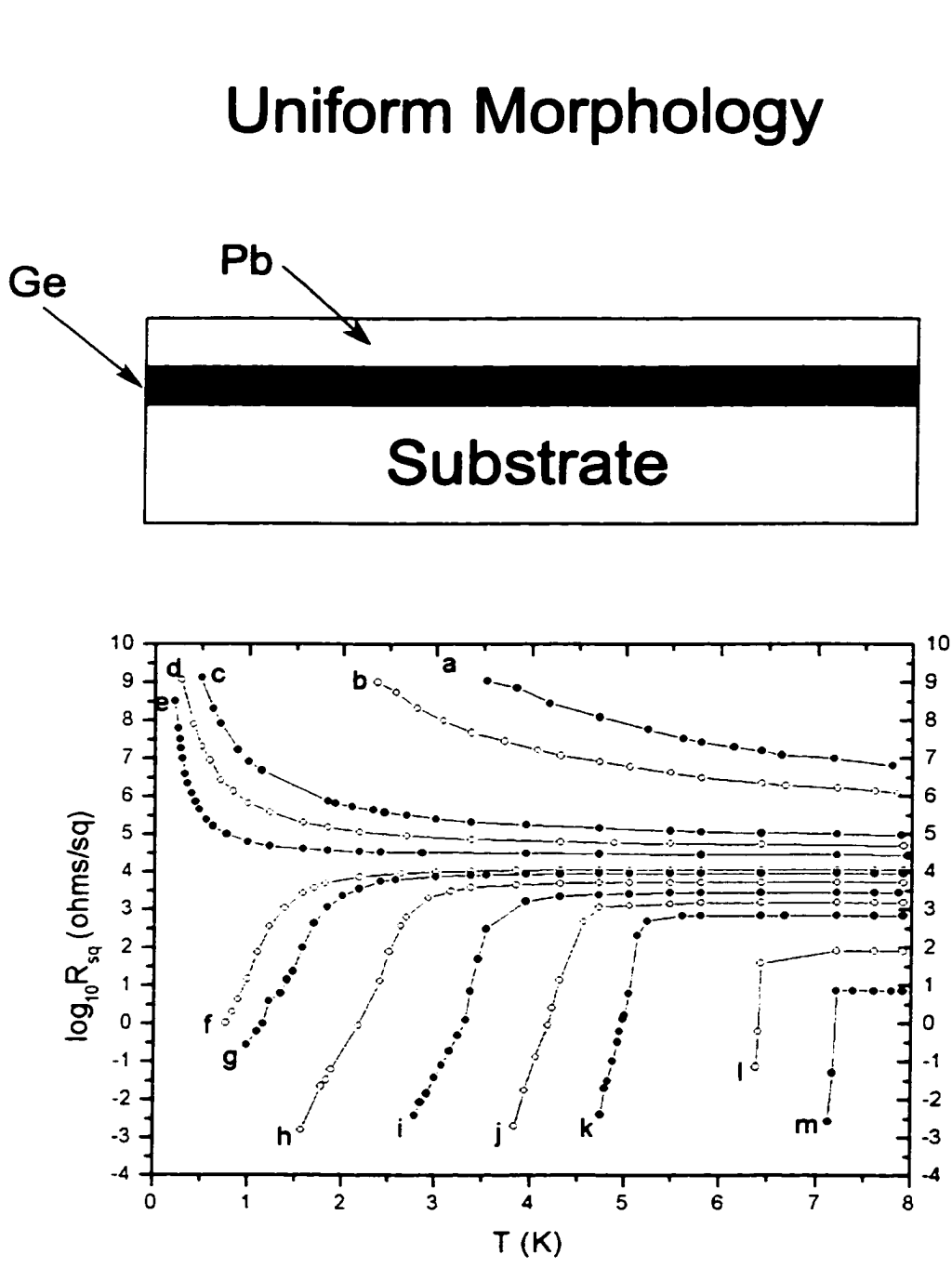

Figure 3.2: Transport of a uniform Pb film

Two-dimensional sheet resistance transport of a uniform morphology formed by deposition of Pb on top of a few monolayers of Ge.

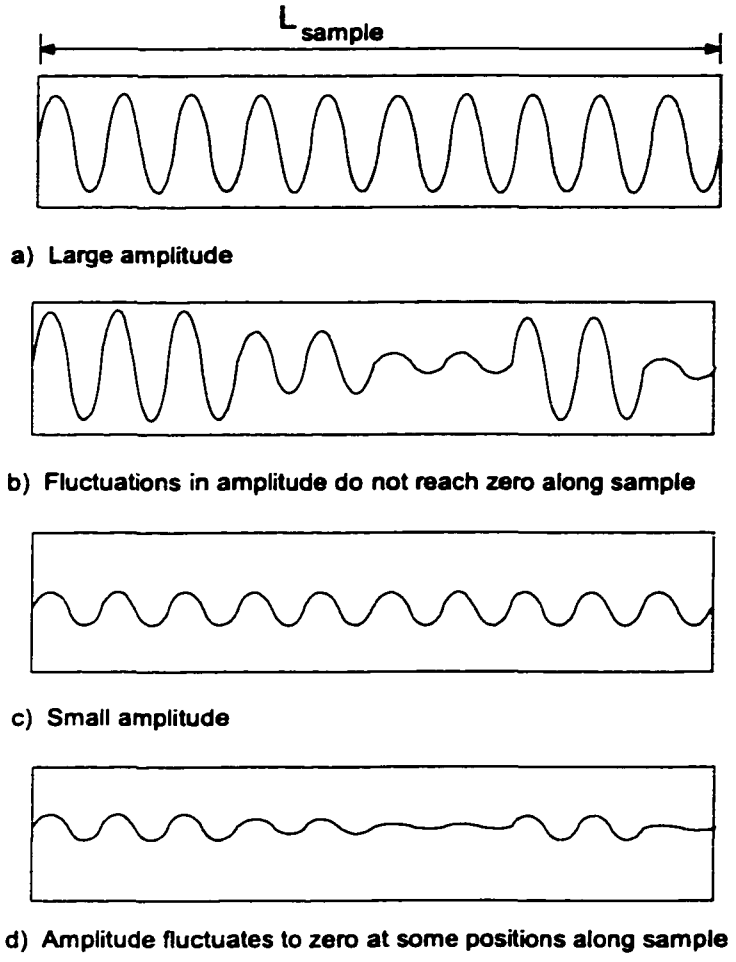

Figure 3.3: Variation in amplitude of superconductor order parameter

(a) Extended wavefunction of defined phase and large amplitude. (b) Extended wavefunction with defined phase but amplitude fluctuations. (c) Extended wavefunction of defined phase and smaller amplitude than that in a. (d) Extended wavefunction of defined phase but amplitude fluctuations that suppress the amplitude to zero at some spots.

are very important at the S-I transition in the uniform morphology. As the temperature is reduced below T_c, more Cooper pairs form, and the order parameter amplitude increases. it becomes more robust against fluctuations.

If there is global phase coherence across the sample as seen in figure 3.3a, the superconducting state may or may not be resistant against amplitude fluctuations. The wavefunction amplitude measures the superfluid density. If the extended wavefunction is susceptible to amplitude fluctuations, superconductivity is destroyed if the amplitude fluctuates to zero. The local amplitude can be small if the local density of Cooper pairs is low. If the amplitude is large enough, these fluctuations won't destroy superconductivity since the amplitude is large enough to withstand amplitude fluctuations up to a certain size as seen in figure 3.3b. If however the amplitude is smaller as in figure 3.3c, amplitude fluctuations can lead to zero amplitude at some local position as seen in figure 3.3d. Amplitude fluctuations to zero result in the superconducting state at that local position fluctuating into a normal state and a resistance resulting.

Compared to the granular films described in the next section, the resistive transitions are much sharper for a uniform film, but there is still an enhanced width to the transition.

3.1.2 Granular morphology

In the granular morphology, grains naturally localize wavefunctions due to their physical and electrical separation and this limits regions of phase coherence. A granular morphology is formed by evaporating a material directly onto a glass substrate with no underlayer of Sb or Ge. Deposited Pb reaches the glass substrate with energy from the hot deposition causing the Pb atoms to move and clump in the formation of grains. The binding is weak and is probably Van der Waals. Smaller grains form on a substrate held at 10 K than one at room temperature. Thus if grains evaporated at 10 K are warmed to room temperature, the grains will coalesce and destroy their original configuration. A two-dimensional granular

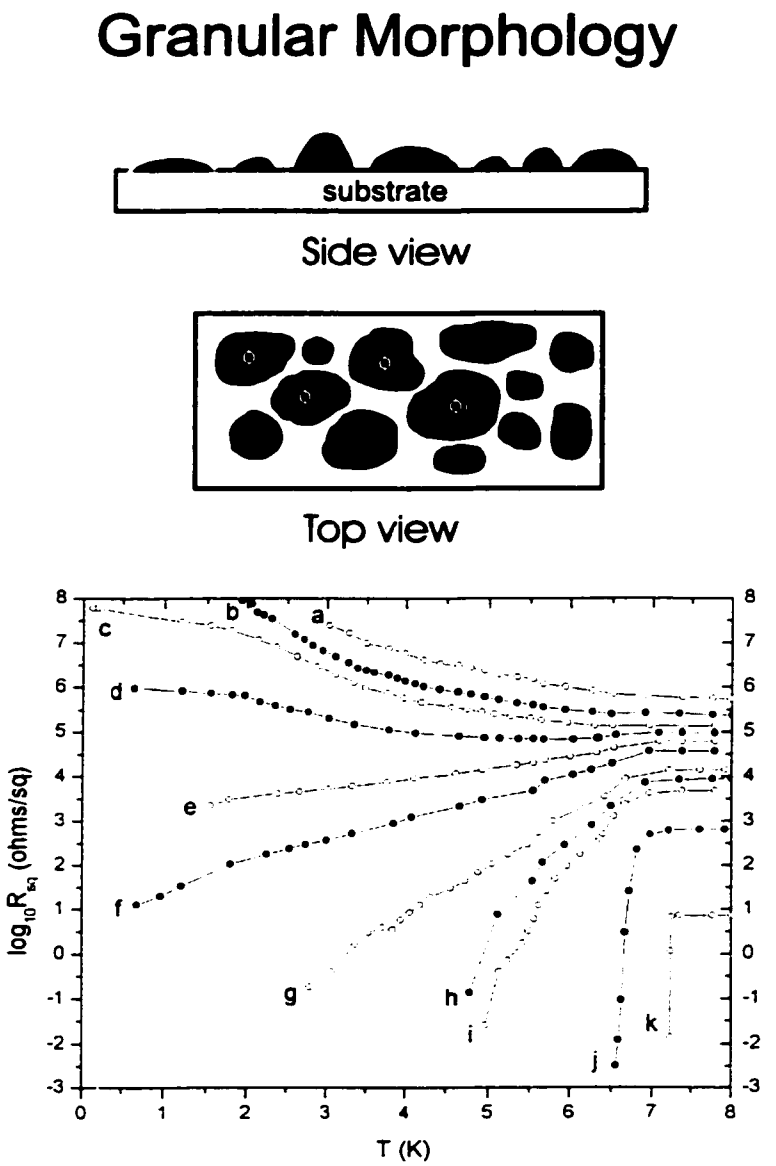

Figure 3.4: Transport of a granular Pb film

Two-dimensional sheet resistance transport of a granular morphology of quench-condensed Pb.

film of Pb quench condensed onto a 10 K substrate will be electrically continuous at 90-100 Angstroms. The film shows activated insulating behavior when it is first electrically continuous. The sheet resistance transport is shown in figure 3.4 along with a cartoon of the granular morphology.

As will be shown in Chapter 4, experiments in this thesis show that Pb grains in an insulating film are superconducting with a full BCS energy gap. Thus the order parameter amplitude is not suppressed from the bulk value of Pb. The granular film can be thought of as a random array of resistively shunted Josephson junctions. This configuration is very interesting because both a quasiparticle current and a Cooper pair current are simulataneously important in determining the sheet resistance behavior of the granular film. The transport is thermally activated insulating behavior, and yet the disorder leading to an insulating state does not inhibit local superconductivity. This contrasts to the uniform morphology where the energy gap is zero in the insulating state.

When first electrically continuous, the wavefunctions are phase coherent over some region smaller than the sample length: each region has a different phase, but the wavefunctions don't overlap to allow conduction other than activated quasiparticle hopping [see figure 3.5a]. Not until more Pb is deposited do wavefunctions overlap and act as Josephson junctions. Cooper pairs are transferred between regions, but it is not enough to lock phase. The film is now in a state of weakly overlapping wavefunctions of different phase as seen in figure 3.5b. Because the overlap is not large, the global wavefunction is susceptible to fluctuations. Phase fluctuations result in 2π phase slips and a non-zero time averaged voltage across the film when current is applied. With further deposition of Pb, the film gradually reaches an extended state of global phase coherence as seen in figure 3.5c. Only when there is global phase coherence does the film exhibit superconducting behavior below some transition temperature.

The transition from insulating behavior of separated superconductor wavefunctions to overlapping wavefunctions takes place at a larger normal state sheet resistance value than that of a uniform Pb film. For a range of normal state sheet

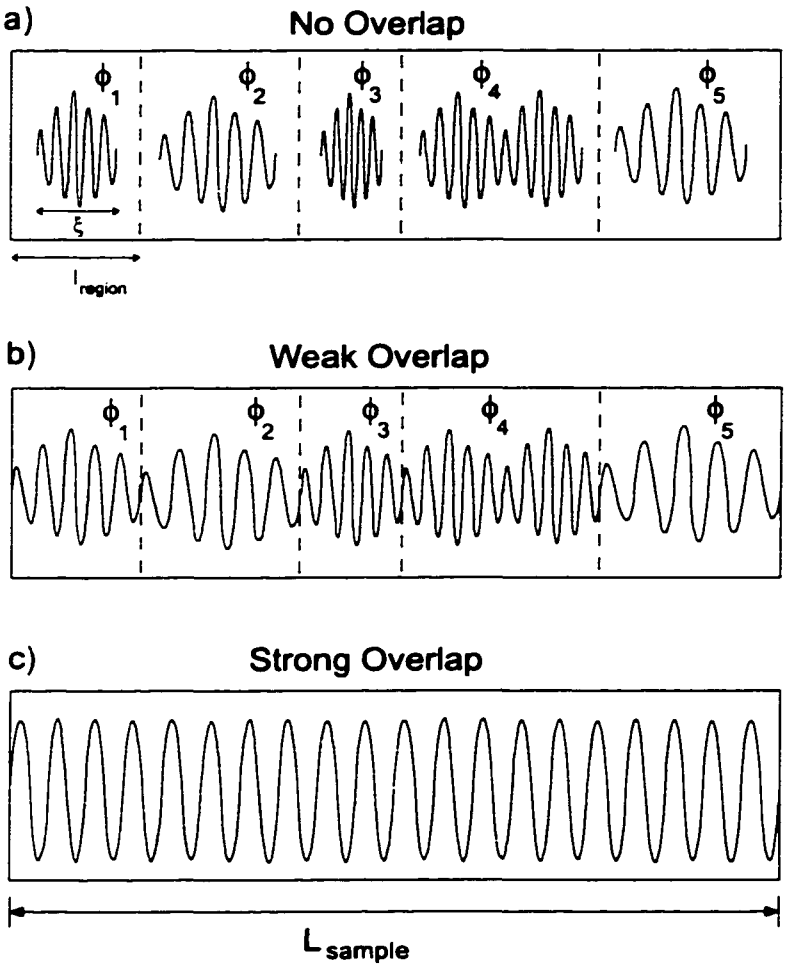

Figure 3.5: Pictoral diagram of overlapping superconducting wavefunctions

(a) No overlap of wavefunctions between regions leads to insulating behavior. (b) Weak overlap of wavefunctions leads to long resistive tail behavior. (c) Strong overlap of wavefunctions leads to global phase coherence and long range superconducting behavior.

resistance, superconductor wavefunctions are overlapping in a granular system and exhibiting wide resistive transitions while superconductor wavefunctions in a uniform system do not exist yet because the amplitude is suppressed to zero.

Once wavefunctions exist and overlap, the transition temperature is only suppressed to 7.1 K in granular films as opposed to the severe suppression seen in uniform films. In the weakly overlapping region, the resistive transition is very broad. Apparently phase fluctuations are very severe and do not allow a globally phase coherent state to occur in the range of temperatures experimentally measured. The resistive tails show interesting e^T behavior. This is odd because most behaviors in nature occur as $e^{1/T}$. As the normal state sheet resistance is reduced, the resistive tails occur over smaller temperature ranges, but T_c of the individual grains is still at 7.1 K. Thus the BCS mean-field temperature is nearly the bulk value of Pb for the granular films, while phase fluctuations prevent all Cooper pairs from coupling into a common phase state.

3.2 Experimental Methods

3.2.1 Sample preparation

An insulating substrate was prepared at room temperature with gold contacts and an oxidized Al base electrode for tunneling, and then the material of interest was later thermally evaporated in an ultrahigh vacuum at cryogenic temperatures. The substrate, a glass slide, was cleaned by alternately rinsing in distilled water and dunking in the following: soapy distilled water, acetone, and isopropyl alcohol. After drying the slide with Nitrogen gas, the slide was firepolished on a piece of quartz. Thin gold contacts less than 100 Angstroms thick were evaporated on top of a few monolayers of Ge in a vacuum bell jar system at a pressure around $3x10^{-6}$ Torr. The glass substrate with gold contacts was then placed on a copper sample block and thermally sunk with Apeizon L-grease. Small gold wires were silver-painted to the Au contacts for electrical contact between the sample block

and the substrate. An Al base electrode with a trace (ppm) of Mn impurities was then thermally evaporated onto a shadow mask covering the substrate in a vacuum bell jar system at a pressure around $3x10^{-6}$ Torr. The Mn impurities are included in the Al to guarantee a normal base electrode for tunneling measurements. The completed room temperature configuration is shown in figure 3.6. After venting with Nitrogen gas, the Al-Mn base electrode was oxidized for 24 minutes at room temperature to form a suitable oxide barrier for tunneling measurements. The tunnel junction resistance is of the order of $10^5 - 10^6$ Ohms with this oxidation time. The shadow mask for a stripe of material to be evaporated later was placed on the substrate and the sample head was placed in a measurement device. To prevent further oxidation of the Al-Mn stripe, the measurement device was pumped out and immediately placed in liquid Nitrogen.

This measurement device was either a He3/He4 dilution refrigerator surrounded by a vacuum can where the sample block is thermally linked to the mixing chamber, or the device is a simple insert stick surrounded by a vacuum can where the sample block is thermally linked to the vacuum can. This stick is immersed in liquid ^{4}He. The arrangement of the substrate with respect to the source materials to be evaporated is shown in figure 3.7. Both the dilution refrigerator and the simple stick are placed in a dewar filled with liquid Helium. The advantage of the dilution refrigerator is its capability of reaching temperatures as low as 100 mK, while the simple stick can only reach 1.7 K by pumping on the helium bath. A dilution refrigerator is explained in more detail in Richardson [25]. The dilution refrigerator has a shutter enabling the sources to be heated without depositing material onto the substrate. The simple stick does not have a shutter. Both have a 5 MHz quartz crystal to monitor average thickness of material deposited. The tooling factor was calibrated by measuring a change in frequency and a known quantity of material deposited [22]. The dilution refrigerator was used in the quench condensed granular Pb film experiments in chapter 4, but was not reliably working for any further experiments.

Increasing the film thickness is easily achieved by having a source of material

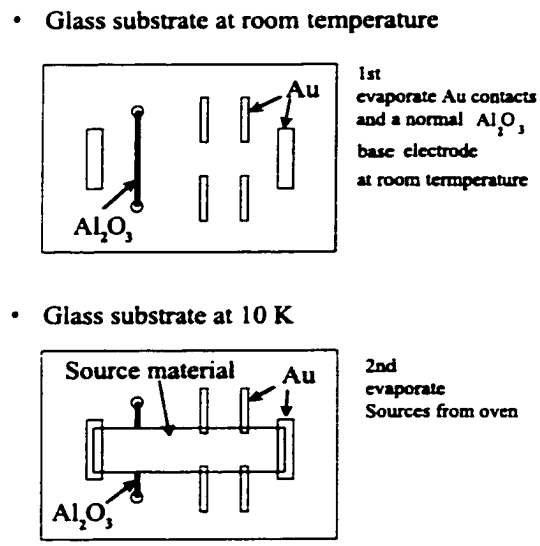

Figure 3.6: Substrate configuration

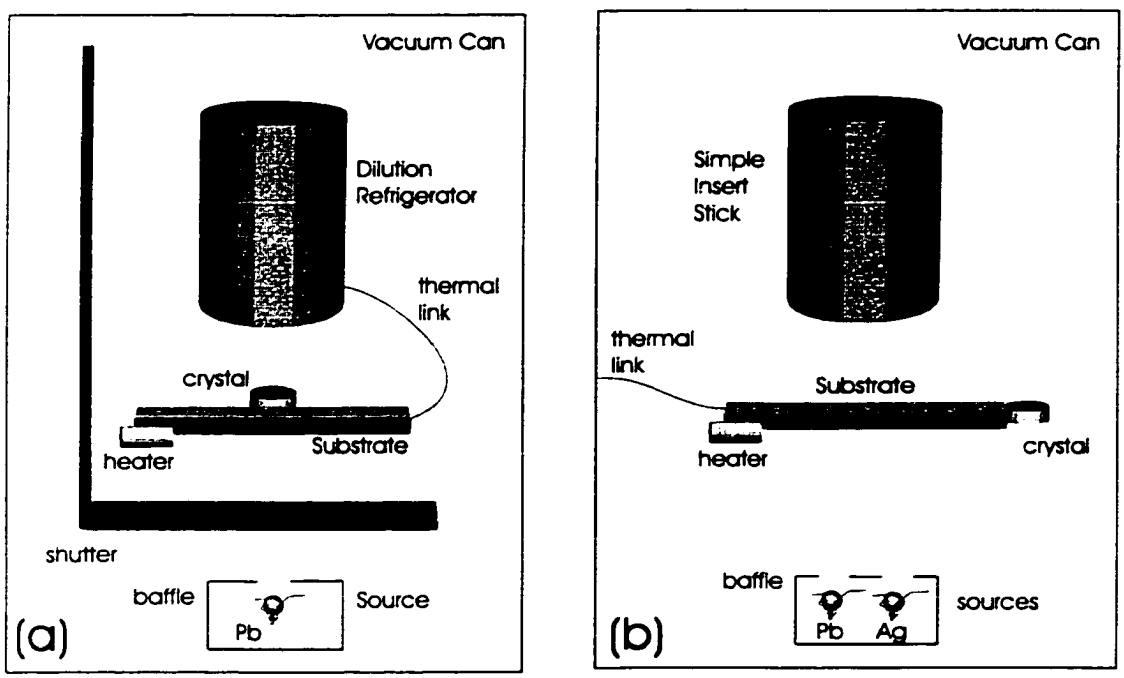

Figure 3.7: Measurement devices

(a) Configuration of dilution refrigerator. (b) Configuration of simple insert stick.

to evaporate. Tungsten wire is wrapped into a basket form to hold Pb or Ag for evaporations. For evaporating Sb, tantalum wire was used. Each basket was attatched to electrical current posts on an electrical feedthrough referred to as an oven. With four posts, up to three baskets can be used for independent source evaporations. The sources were pre-melted at room temperature to form a ball of material that would stick to the basket and to limit oxidation of the sources which is important when there is no shutter as in the simple stick. The dilution refrigerator has a shutter which allows for evaporation of the sources without worry of any material reaching the substrate. Even without a shutter, there is good control of the amount of material deposited as long as the rate is not too quick. When the sources are evaporated, the substrate is held at 10 Kelvin via a heater in the sample block. The substrate is about 3 inches form the sources. The vacuum can in a helium bath allows any stray gasses to be cryopumped to the walls, thereby guaranteeing a reasonably pure film. The sources can get quite hot when they are evaporated, and so a copper baffle sunk to the helium bath is placed over them to limit the temperature rise of the substrate to a few degrees.

3.2.2 Measurement Techniques

Because two dimensional films are sensitive to RF noise, all measurements are done in a RF screened room with analog equipment except for the digital crystal thickness monitor. The crystal monitor is only on during depositions, however, and not during transport and tunneling measurements. The temperature of the two-dimensional film is varied during the measurements, and this affects the sheet resistance. To monitor the temperature, a calibrated RuO thermometer is used with the dilution refrigerator and a calibrated Cernox thermometer is used with the simple insert stick. See Richardson [25] for more information. A simple carbon resistor acts as a heater. A bridge technique is used to measure thermometer readings. This is illustrated in figure 3.8. An analog resistor box, an analog Lock-In (PAR model 124A, 2Hz-210kHz), and two pre-amps (Ithaco 1201) were

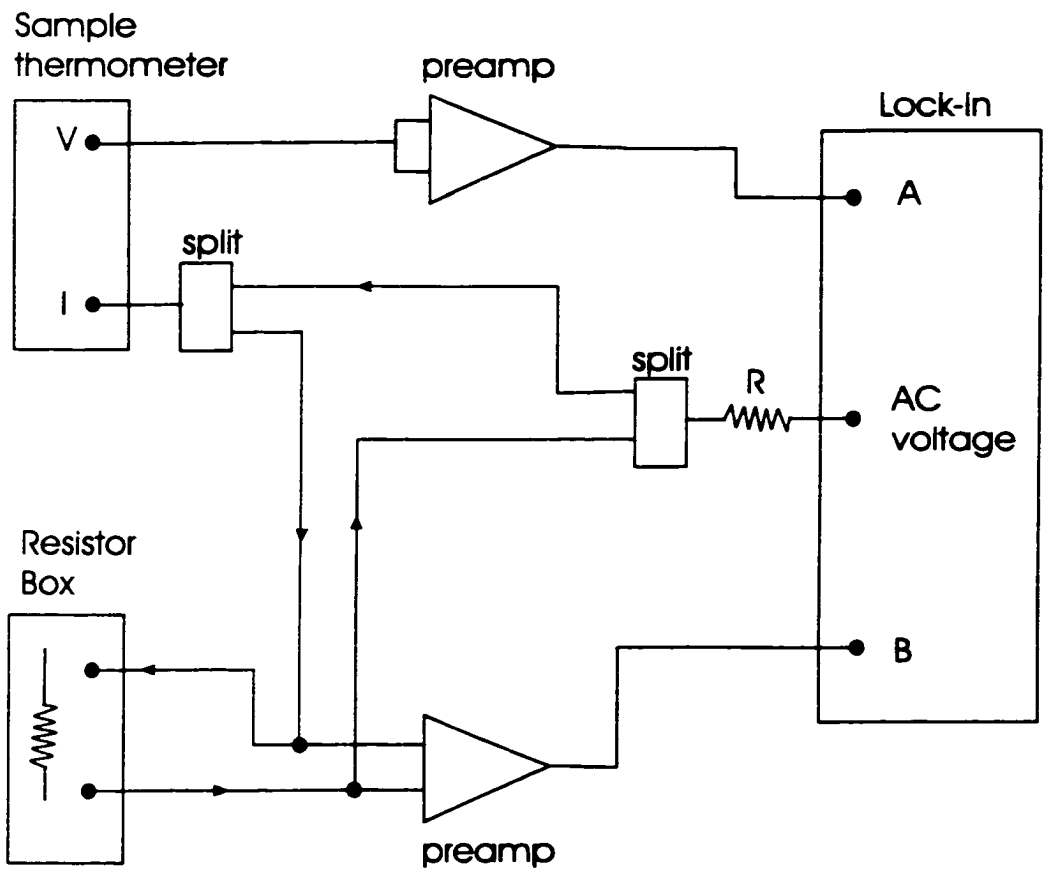

Figure 3.8: Block diagram of thermometry measurement

used to form the bridge where the lockin read zero when the resistor box matched the thermometer value. The lock-in provided an AC voltage of 1 Volt and was passed through a 10^6 Ohm resistor for a current to pass through both the sample thermometer and the resistor box. A frequency of 27 Hz is used to monitor input from the resistor box and the thermometer. To zero out capacitance in the signal from the resistor box and the thermometer, the output of the lockin is zeroed at 90 degrees out of phase.

In order to stop the evaporation at a high sheet resistance with insulating properties, a 20 MΩ resistor is placed in parallel with the substrate. With current and voltage leads in a 2-wire configuration, the onset of conduction in the film can be detected when the effective resistance decreases from 20 MΩ. The current and voltage leads are then changed to a 4-wire configuration for an accurate resistance measurement of the insulating film. Further depositions can tune the film through the insulator-superconductor transition. The sheet resistance is measured at each deposition as a function of temperature. At each temperature, an I-V transport measurement is taken. A battery box provides a current through a known precision resistor and is fed to the film, and the current measured through the precision resistor and the voltage drop across the sample is monitored with an X-Y chart recorder. Taking an I-V transport measurement at each temperature ensures that the most accurate sheet resistance value will be attained. Only the linear Ohmic part of the I-V characteristic is used to determine the sheet resistance value at each temperature. Care is taken to use a current small enough such that no heating effects are observed. So that sheet resistance values can be compared from film to film, a resistance per square, R_{sq}, is defined such that each square equals length/width of area measured with a 4-point measurement. For tunneling measurements, the normal state value is divided out to normalize all the tunnel I-V plots for various normal state sheet resistances. This way, the tunnel junctions can be compared since they all have the same Al-Mn base electrode and oxide barrier.

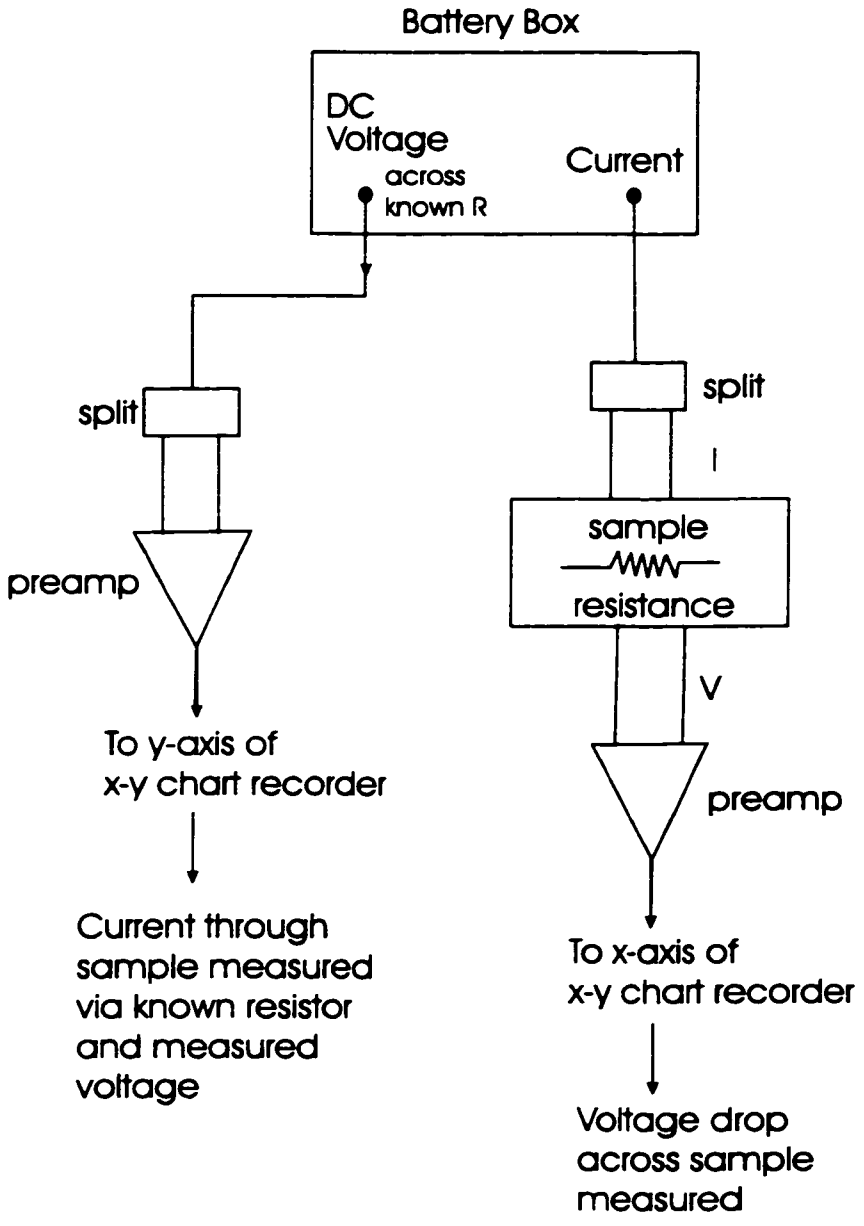

Figure 3.9: Block diagram of sample I-V measurement

Chapter 4

Quench condensed granular Pb films

4.1 Introduction

Using the experimental procedures described in chapter 3, we studied the superconductor-insulator transition in two-dimensional quench condensed granular Pb films with an emphasis on the insulating side. The films are disordered, and thus inelastic scattering affects the normal state conductance and as explained in chapter 2, the lifetime of a Cooper pair is shortened. Lifetime effects are detected via density of states measurements where the gap edge is broadened by some lifetime broadening factor, Γ. Experiments by Dynes [9] probing the density of states in two-dimensional quench condensed granular Al films near the S-I transition found that Γ linearly increased with increasing sheet resistance. An extrapolation predicted the lifetime broadening factor would approach the energy gap and lead to strong suppression of superconductivity. It was proposed that Γ increasing as normal state sheet resistance increases drives the S-I transition. Granular films with insulating transport are strongly disordered in an S-I transition, and so lifetime broadening was thought to be a major contributer to the insulating state below T_{MF}. The density of states was not probed, however, for the insulating film.

We probed the density of states of quench condensed granular Pb films and found that the energy gap, Δ, on the insulating side of the transition is not completely smeared out, but is in fact equal to the BCS value of bulk Pb with some lifetime broadening. The lifetime broadening factor, Γ, is within 3-7 percent of the bulk energy gap, and is clearly not close to approximating the gap size. Thus, with insulating transport, the grains are large enough to support superconductivity, but they are not close enough to support Josephson coupling. Josephson coupling is very important in granular films as it allows superconducting wavefunctions to couple and if the coupling is strong enough, phase fluctuations are suppressed. As discussed in chapter 2, suppression of phase fluctuations is critical for a long range superconducting state. When phase fluctuations are not suppressed, sheet resistance properties can be qualitatively explained by a two-dimensional array of resistively shunted Josephson junctions undergoing 2π phase slips.

A glass substrate with gold contacts was used as described in chapter 3, and the benefits of this layout is that both transport and tunneling measurements can be made on the same film. An added benefit is that the same base electrode and oxide barrier is used as the film thickness is varied so comparisons can be made between these films. A He3/He4 dilution refrigerator was used for *insitu* evaporations of Pb onto a glass substrate held at 10 K. Electrical continuity with a resistance around one $M\Omega$ was achieved at approximately 100 Angstroms of mean thickness Pb. With just a few additional Angstroms of deposited material, the film was tuned from an insulating state into a quasireintrant state, and from there into a long resistive tail state (see figure 4.1). A globally superconducting film with a sharp transition requires an additional 100 to 200 Angstroms from the initial mean thickness of the insulating film. The sheet resistance measurements are experimentally limited by noise, non-linearity, and/or temperature, and so the sheet resistance is measured as close to zero Kelvin as experimentally possible.

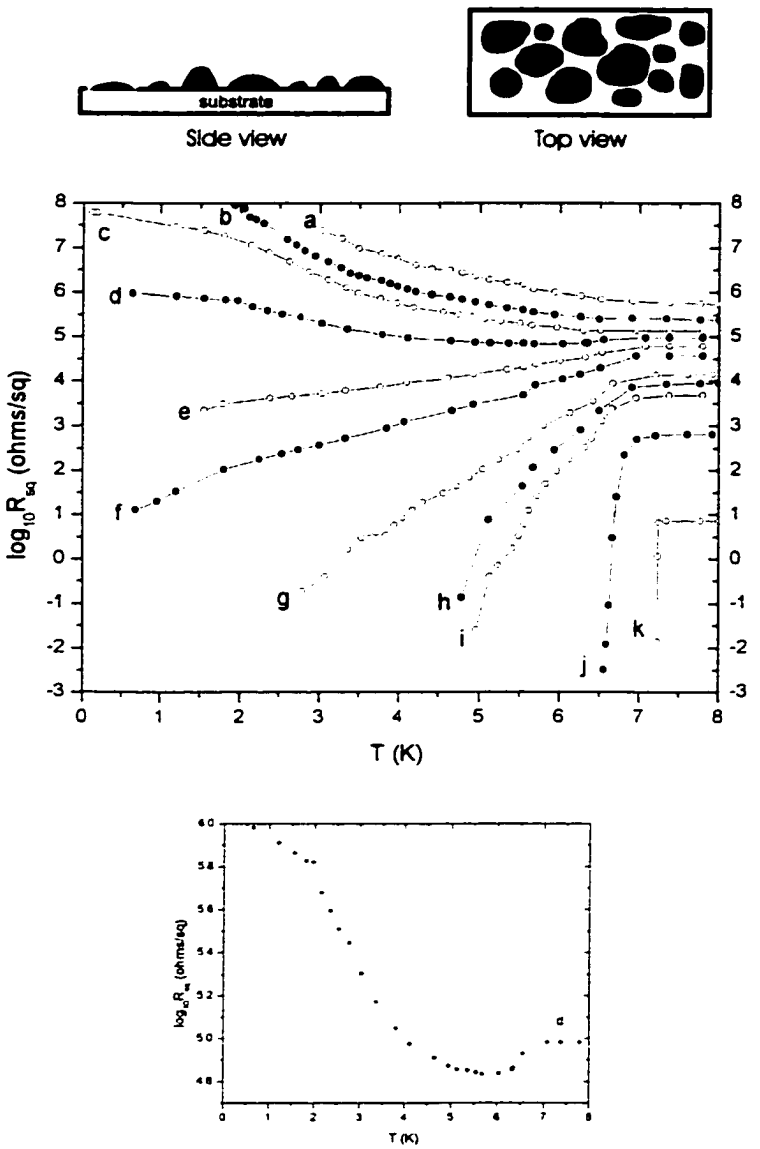

Figure 4.1: Granular morphology and corresponding transport data

Quench condensed granular Pb morphology leads to grains of varying phase and coupling strengths. Resistive transport is shown on a log plot and curve c is plotted on a smaller scale to show features of quasireintrance. The lines are a guide to the eye in the transport plot.

4.2 Results

We measured transport for a range of normal state sheet resistance varying from 10^6 Ohms/sq down to 10 Ohms/sq as shown in figure 4.1. This data spans over four orders of magnitude using the same substrate and the same tunneling base electrode and barrier. As 100 mK is approached, the sheet resistance at different film thicknesses varies from 10^8 ohms to 10^{-3} ohms. This is over 12 orders of magnitude and requires a log plot to show the entire S-I transition of the transport data. The transition temperature T_{MF} is not clearly defined by a sharp transition, and so it is defined to be the temperature at which the resistance is half the normal state sheet resistance. Remember that figure 4.1 is a log plot, and so half the normal state sheet resistance on a linear plot appears near the knee of the resistive transition in the log plot of figure 4.1. The film T_c occurs when the sheet resistance is zero. Of course on a log plot, the sheet resistance will not appear to go to zero. From the plots, it is not clear if or when this is achieved to the limit of our measurements, but it does appear that the sheet resistance is headed toward zero.

Above about 10^5 ohms, the transport is insulating and the sheet resistance increases with decreasing temperature and follows activated behavior. This is indicative of a strongly localized state. For curve b in figure 4.1, we found activated behavior with an activation energy of 1.46 meV which is close to the superconducting energy gap measured of 1.43 meV. This is shown in figure 4.2. Below about 10^5 ohms, the transport has long resistive tails. This is indicative of a weakly localized state. A sharp transition indicates an extended state with global phase coherence. See chapter 3 for more details. Around 10^5 ohms, there is an interesting sheet resistance behavior called the quasi-reintrant state which is a competition between global superconductivity and strongly localized behavior as seen in curve c of figure 4.1. Below T_{MF}, the sheet resistance of a quasi-reintrant curve decreases below the normal state resistance value as the superconducting wavefunctions of each grain try to phase lock, but, at some temperature below T_{MF}, the sheet resistance

increases with decreasing temperature as in strongly localized behavior.

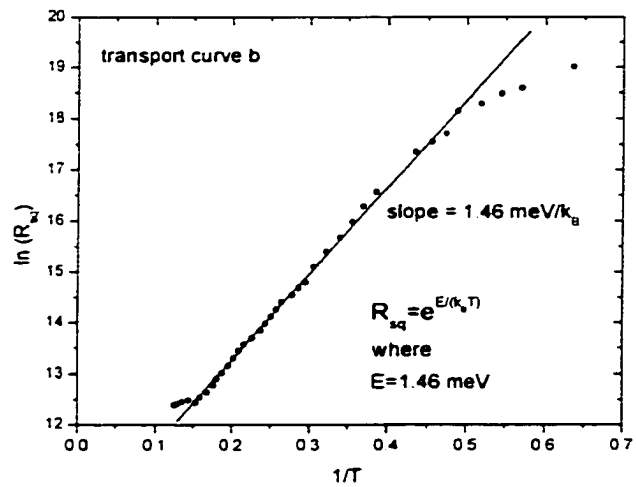

Figure 4.2: Activated transport

Plot b of the previous transport figure is fit to $R_{sq} = e^{E/kT}$ where E is an activation energy.

The sheet resistance varies with temperature in the long resistive tails of the weakly localized region according to the relation log(R)=log(R_N) + mT where R_N is the normal state sheet resistance above T_{MF} and m is the slope of the resistive tail on a log R versus T plot. Normal state properties are very important in determining superconducting properties below T_{MF}. As the normal state sheet resistance decreases, the coupling between grains increases and thus the slope increases. The T_{MF} for these long resistive tails all occur at 7.1 K which is slightly below the bulk Pb value of 7.2 K. It is not clear whether the long resistive tails will approach zero sheet resistance or some non-zero sheet resistance value as 0 Kelvin is approached.

Tunneling I-V curves for junctions on films b, h, and k at 2.11 K were normalized with their respective normal state tunneling curves at 8 K and are plotted in figure 4.2. Both the data and a BCS fit are shown in this figure. These tunnnel-

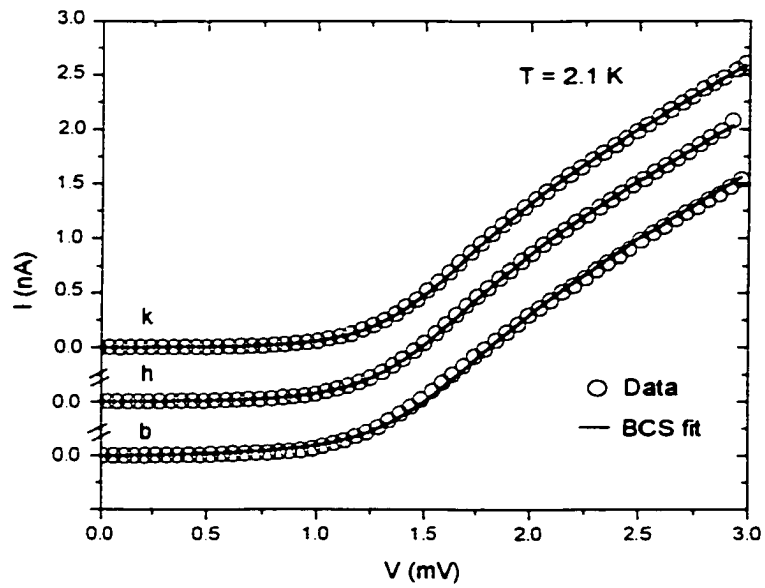

Figure 4.3: Tunneling I-V at 2.1 K for characteristic granular Pb transport films

Tunnel I-V for quench condensed granular Pb film of insulating transport, weakly localized transport, and extended transport at 2.1 K. Open circles are data for tunneling into films b, h, and k of tranport figure. Line is a BCS fit.

ing data indicate superconductor-insulator-normal metal (SIN) tunnel junctions because of the clear indication of the energy gap in the quasiparticle density of states. The agreement between the data and the fit is very good. The tunnel I-V for curve k is for a globally phase coherent film, it is surprising given that curve b is nearly identical to k because it is for an insulating film.

Tunneling into a high resistance film with insulating transport requires a large tunnel junction barrier resistance in order to have a true four-terminal measurement. The tunneling rate of electrons onto the grain must be less than the escape rate of the electrons off the grain in order to guarantee an equipotential across the width of the junction and avoid grain charging effects. The film resistance at 2.11 K is on the order of 10^7 ohms, and would require a junction resistance larger than this. Junction resistances were typically $10^5 - 10^7$ ohms, but this is adequate because the junction aspect ratio, length/width, is 1/10.

Since the tunnel junction resistance was on the order of $10^5 - 10^6$ ohms, it was not feasible to directly measure the density of states with a dI/dV measurement using a standard AC lock-in measurement. Another possible method to measure the energy gap was to take the derivative manually from the measured I-V plot, but this is not the most accurate method because of the way the data was collected. The data was collected using an analog method rather than a digital method. The superconducting energy gap can be measured accurately in an alternative way by fitting a normalized I-V data plot with a computer program using a simplex fitting algorithm. This algorithm was applied toward tunneling I-V data in a computer program written by A. La Porta (A. La Porta was in the Dynes lab at the time of this experiment) which allowed different variables such as Δ, Γ, and temperature to be tuned. The algorithm reduces the error between the normalized I-V data plot and a calculated BCS I-V plot by independently varying these. The BCS tunneling current versus voltage relation used in the algorithm is calculated from the SIN junction equation given in chapter 2. With the temperature fixed, the energy gap Δ and the broadening term Γ were varied in fits of tunneling data taken on curves b, h, and k. The value of the superconducting energy gap found, 1.43 meV at 2.1

K. is equal to that expected from our knowledge of Pb. For film b. values of the broadening parameter, Γ, are only 3-7 percent of Δ. For film h and film k, Γ is only 0.5-3 percent of Δ. This points to the idea that the granular film may be disordered, but the grains are large enough to support superconductivity.

4.3 Relation of Josephson coupling strength to the sheet resistance of a granular Pb film

The sheet resistance properties of the film depend sensitively on the coupling of the grains. The current path in a granular film is a mixture of well coupled grains, poorly coupled grains, and uncoupled grains. As the coupling improves, the normal state sheet resistance is lower. Below the transition temperature T_{MF}, the grains are superconducting with local phase coherence, but if the sheet resistance is non-zero, the film lacks global phase coherence. The superconducting grains act as an array of resistively and/or capacitavely shunted Josephson junctions where the barrier is either a physical separation of the grains, a point contact, or a constriction. The Josephson binding energy, $E_J(T)$, is an important parameter giving a measure of the phase locking ability of two coupled superconductors.

$$E_J(T) = \pi^2 N(0)^2 |M|^2 \Delta(T) \tag{4.1}$$

The normal electron states are localized within a region that includes either one or many grains, and for a current to traverse the film, it must travel from one localized region to the next by hopping or tunneling. The average tunneling matrix element for electron transfer near the Fermi surface is represented by $|M|^2$, and as the coupling improves, $|M|^2$ increases.

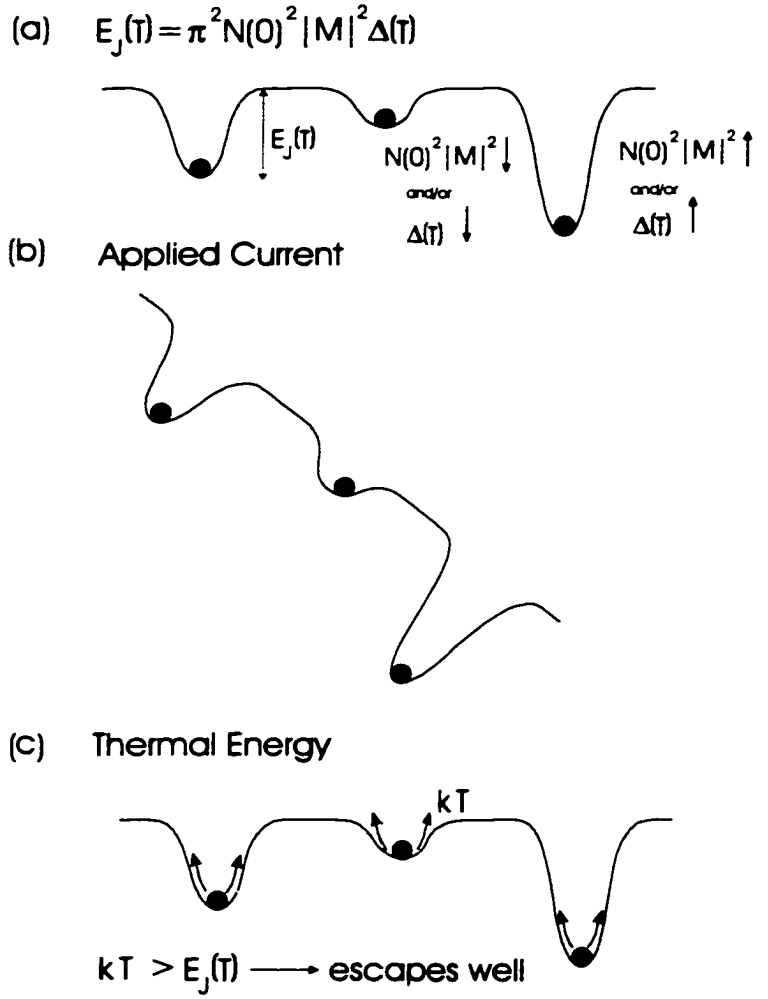

Figure 4.4: Washboard model of a resistively shunted Josephson junction at a variety of well depths.

(a) Figure a shows the relation of well depth, $E_J(T)$, to the coupling, $N(0)^2|M|^2$, and the energy gap, $\Delta(T)$. (b) Figure b shows the effect of an applied current is to tilt the washboard. This effectively reduces the well height on one side, and allows the particle greater chance to escape its well. (c) Figure c shows the effect of thermal energy, kT, is to oscillate the particle in the well. This increases its chances of escaping the well.

4.3.1 Washboard model

The washboard model of a Josephson junction provides a simple picture of how thermal energy, kT, and applied current, I, can affect the phase coupling of a Josephson junction. As mentioned in chapter 2, a resistively shunted Josephson junction can be represented as a ball in a washboard potential of well depth $E_J(T)$. The ball represents the phase difference of the junction, and if the ball escapes the well, a 2π phase slip occurs. The larger $E_J(T)$ is, the deeper the well, and the less likely 2π phase slips are. A supercurrent can then flow between the two superconductors with less chance of voltage spikes from 2π phase slips. The variation in size of $E_J(T)$ is shown in figure 4.4a, and this will be explained more in the next section. The ball can roll out of the well either by thermal excitation or by applied current.

Thermal energy can cause the ball to oscillate in the well, and if the thermal energy kT is larger than the well height of $E_J(T)$, the ball can roll into a neighboring well resulting in a 2π phase slip as seen in figure 4.4c. The smaller the well height E_J, the easier it is for thermal energy to roll the ball over to a neighboring well. The Josephson binding energy E_J increases and the thermal energy kT decreases with decreasing temperature, and thus fewer phase slips occur due to thermal oscillations. An applied current can lower the energy barrier by tilting the washboard as seen in figure 4.4b. When the washboard is tilted at an angle, the well height is effectively reduced on one side, so a thermal energy less then E_J can set the ball rolling. If the washboard is tilted such that the ball is no longer trapped in a well, it can roll along the entire washboard undergoing a 2π phase slip at each well. If the potential wells are not deep enough, 2π phase slips can occur and a voltage drop develops across the film. As the temperature decreases, the thermal energy kT decreases relative to the well depth, and this makes it harder for the ball to escape. Thus, more and more washboards can trap the ball and prevent phase slips. Even if E_J increases as temperature decreases, it may not result in a well deep enough to prevent temperature, applied current, or quantum

fluctuations from rolling the ball out of the well. Thus a finite sheet resistance could result as 0 Kelvin is approached.

4.3.2 Factors determining size of $E_J(T)$

The current path of quasireintrant transport and long resistive tail transport contains weakly and strongly coupled Josephson junctions. The properties of a restively shunted Josephson junction are closely tied to the quasiparticle current connecting the two superconductors. Before phase coherence of the two superconductors is achieved via a supercurrent, the quasiparticle conductance, and the energy gap determine how well the superconductor wavefunctions can couple. As the temperature decreases and phase coherence is not achieved via a supercurrent, a new value of the quasiparticle conductance must be used.

The Josephson binding energy $E_J(T)$ varies via the product of $N(0)^2|M|^2$ and $\Delta(T)$. The factor $N(0)^2|M|^2$ is the total quasiparticle conduction, $G_{q.p.}^{total}(T)$, at the temperature that the Cooper pair channel is large enough to transport a supercurrent which can equalize the phase of the two superconductors composing the junction. If a supercurrent flows, but it is not large enough to equalize the phase, the value of $N(0)^2|M|^2$ used is at the temperature T where $E_J(T)$ is evaluated. Thus the value of $G_{q.p.}^{total}(T)$ used to determine $E_J(T)$ is not necessarily the value at T_{MF}.

As the temperature varies, so does the quasiparticle conduction. If the physical separation is too large, the superconducting order parameters of each grain can not couple, and so Cooper pairs do not pass from grain to grain. In this case, current can only be transferred by quasiparticles, and as the temperature decreases toward zero, there are fewer quasiparticle states to tunnel to at low voltage bias (the energy gap, $\Delta(T)$, is increasing as T goes to zero). Quasiparticles, unlike Cooper pairs, can thermally hop from grain to grain via thermally activated transport. The resistance varies as $e^{E/kT}$ where E is an activation energy. For quasiparticle tunneling, the conductance depends on the number of quasiparticles available and

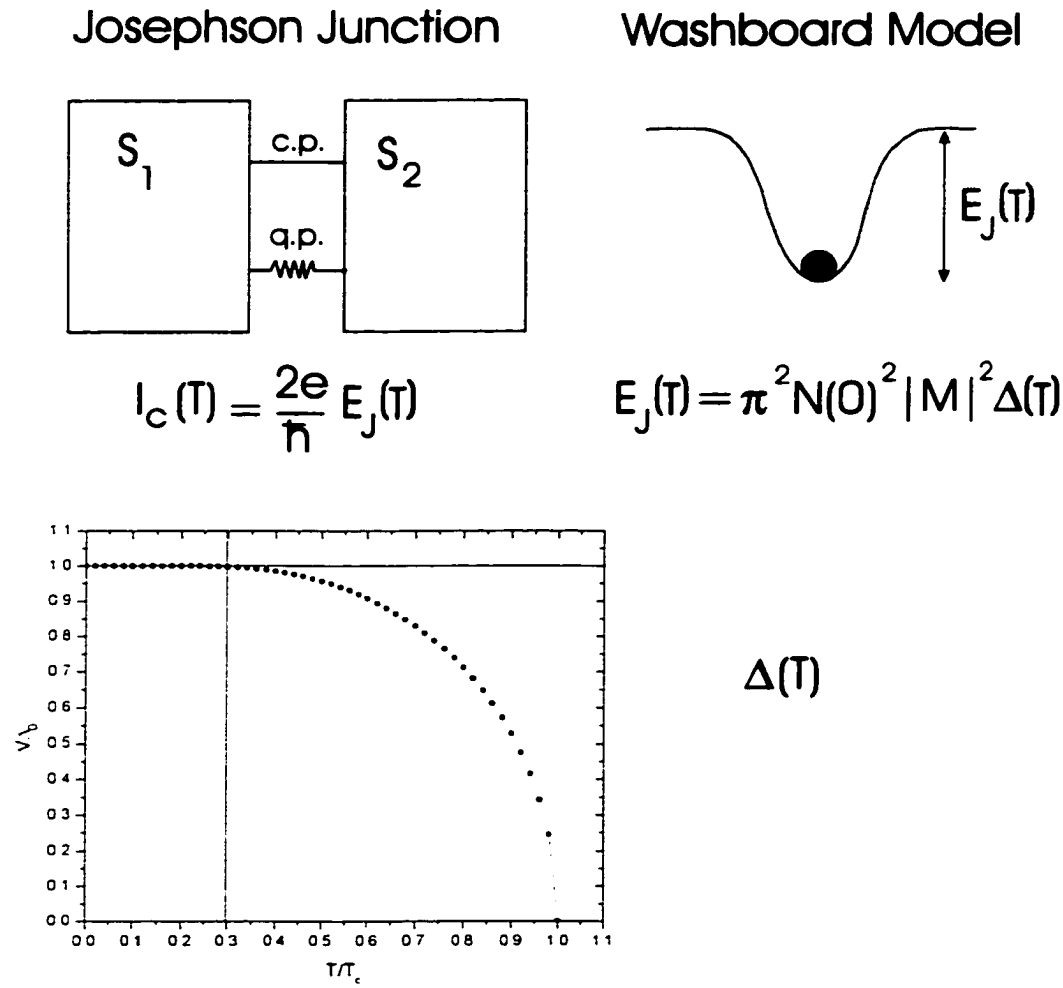

Figure 4.5: Temperature dependence of Josephson binding energy $E_J(T)$

Relation of Josephson binding energy $E_J(T)$ to energy gap $\Delta(T)$ and the overlap of superconducting wavefunctions.

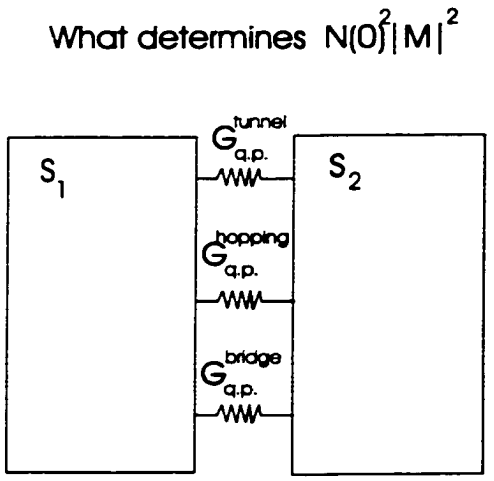

Figure 4.6: Quasiparticle conductance across a resistively shunted Josephson junction

The quasiparticle conductance across a resistively shunted Josephson junction is composed of three general types which shown here are hopping conductance, tunneling conductance, and conductance across a bridge.

the number of tunneling states available. As the grains become superconducting, an energy gap opens up in the density of states, and this reduces the number of quasiparticle states available at low voltage bias. If there is a bridge between the superconductors composed of a constriction or other quasiparticle path, the quasiparticle conduction depends on the number of quasiparticles and the disorder in the bridge. Both quasiparticle transport mechanisms result in increasing sheet resistance as the temperature is lowered, and hence insulating transport behavior. $E_J(T)$ either shrinks or grows due to normal state conductance shrinking or growing with decreasing temperature. The Josephson binding energy $E_J(T)$ also grows due to $\Delta(T)$ increasing with decreasing temperature, but at about $0.3T/T_c$, as seen in figure 4.5, the energy gap saturates at its zero temperature value, Δ_0. At the point where $\Delta(T)$ saturates, $E_J(T)$ is temperature dependent only on $G^{total}_{q.p.}(T)$.

4.3.3 Binding energy affected by phase fluctuations

The binding energy of overlapping superconducting order parameters in a Josphson junction is $E_J(T)cos(\Delta\phi)$ where $\Delta\phi = \phi_2 - \phi_1$ is the phase difference between the two superconductors composing the Josephson junction. If the phase difference is zero, the binding energy is at the maximum value of $E_J(T)$. Phase fluctuations for which $\Delta\phi$ is non-zero will result in a smaller value of binding energy than $E_J(T)$. Thus, the effective well depth in a washboard potential is smaller than $E_J(T)$, and the junction is more susceptible to 2π phase slips.

Cooper pairs need to be transferred at a high enough rate between the two superconductors in order for them to come to a common phase. The Cooper pair transfer rate, Q, is the number of Cooper pairs per unit time that can cross from one superconductor to the next. If Q is large enough, the uncertainty in ΔN is large, and if ΔN is sufficiently large, the phase can be defined. This is according to the uncertainty relation between particle number and phase, $\Delta N \Delta\phi \sim \hbar$. This is illustrated in figure 4.7.

The critical current, $I_c(T)$, of a Josephson junction is the maximum supercurrent that can flow between two superconductors composing the junction. This limits the number of Cooper pairs per unit time that can cross from one superconductor to the next. Since the criticql current limits the Cooper pair transfer rate Q, it can be thought of as a diameter of a channel that controls flow rate. The larger $I_c(T)$ is, the larger Q is, and hence the larger ΔN is. This all results in less susceptibility to phase fluctuations. The critical current is related to $E_J(T)$ through the following equation.

$$I_c(T) = (2e/\hbar)E_J(T) \tag{4.2}$$

Thus, anything discussed in the previous sections that increases the Josephson binding energy $E_J(T)$ will also increase $I_c(T)$, and hence reduce phase fluctuations. Fluctuations in phase prevent phase coherence between the two superconducting regions.

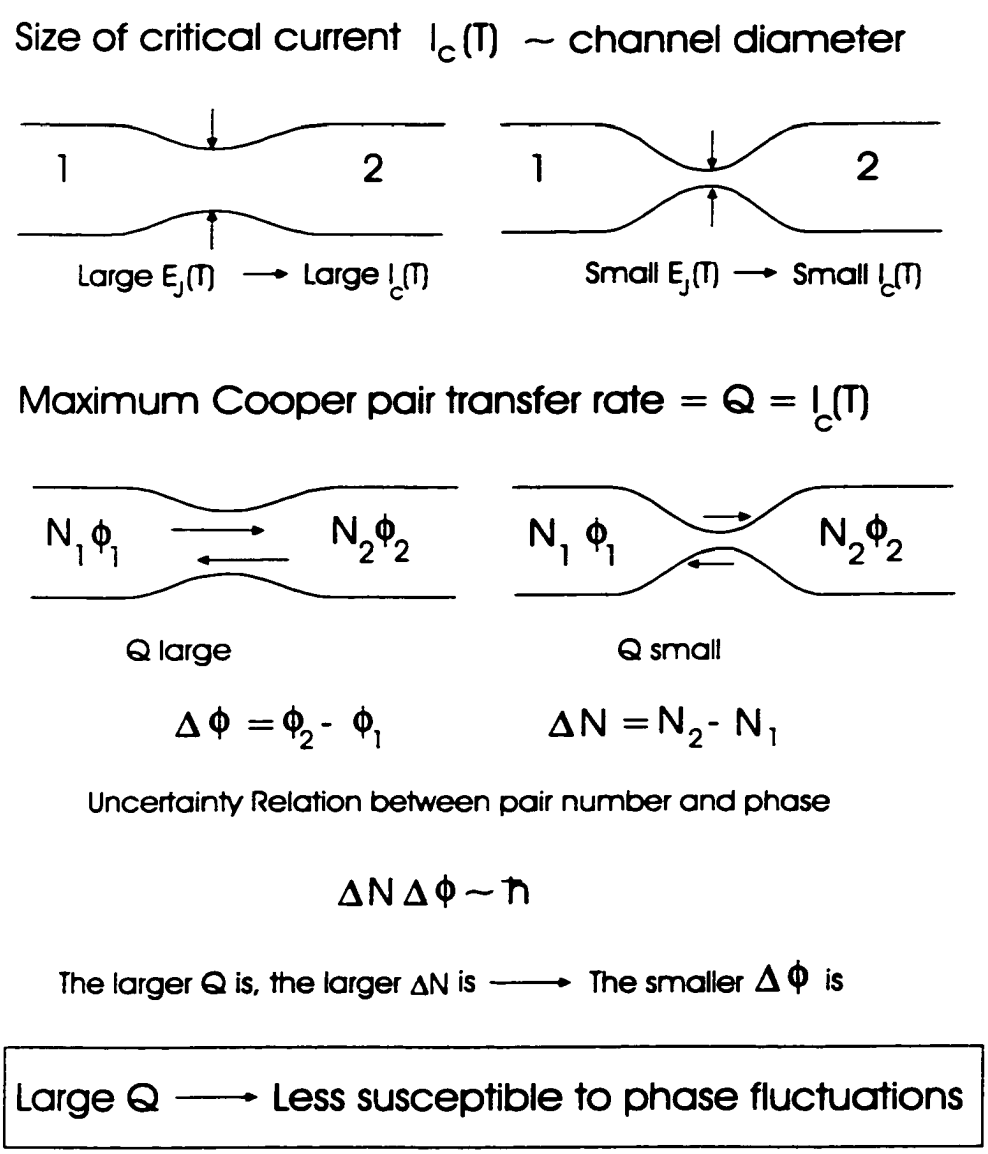

Figure 4.7: Cooper pair transport rate effect on phase.

4.4 Discussion

The lifetime broadening factor, Γ, was not expected to be so small relative to the superconducting energy gap as the normal state sheet resistance, R_n, increased. From experiments on granular Al by Dynes [9], it was expected that the linear relation between Γ and R_n on the superconducting side of the S-I transition would continue on the insulating side. From an extrapolation of measured values, Γ was expected to approach the value of Δ on the insulating side. This seemed likely since the increased disorder leading to insulating transport also results in an increased inelastic scattering rate. An increased inelastic scattering rate directly influences Γ in that the lifetime of Cooper pairs is shortened. Since the measured values of Γ for a granular Pb film were so small, the grains themselves must be large enough for nearly bulk superconducting properties. Cooper pair lifetime is shortened, but not by very much as seen from values of Γ only at 3-7 percent of Δ. If Γ was of the order of Δ, such severe inelastic scattering would destroy superconductivity. The data shows that granular Pb films do not localize electron wavefunctions severely enough with inelastic scattering to destroy superconductivity. In fact, the tunneling data shows that the grains are large enough to locally support superconductivity. Thus, the S-I transition is driven by phase fluctuations and not amplitude suppression.

The range in binding energy from the various coupling strengths can be thought of as a series of washboard of varying well depths. A large normal state sheet resistance between two grains results in a small Josephson binding energy, E_J. Phase fluctuations lead to 2π phase slips and a non-zero voltage drop. This results in the non-zero sheet resistance seen in the long tail region of the S-I transition. As the temperature decreases, E_J increases, and this limits the number of phase slips. More and more grains become locked to a common phase as the temperature is lowered and the area of local phase coherence increases. For curves e,f, and g, the sheet resistance does not appear to be headed toward zero. Thus, the coupling is not strong enough to prevent phase fluctuations from occurring.

4.5 Conclusion

The granular film of Pb proved to be more apt to studying phase fluctuations than previously thought since the grains are fully superconducting even with insulating transport. Thus, Josephson coupling can be explored through the S-I transition from no coupling, to weak coupling, and to strong coupling. Josephson junctions are simply explained with a washboard model where the well depth is very important in determining whether there are 2π phase slips or not. The sheet resistance of the film can be reduced to a consideration of binding energy and Josephson binding energy $E_J(T)$.

Chapter 5

Quench condensed granular Pb/Ag films

5.1 Introduction

In this chapter, we investigate the S-I transition in quench condensed granular Pb films with a normal metal deposited on top to improve the coupling between the superconducting grains. Measurements are taken as we move the film from an insulating state with local regions of superconductivity to a superconducting state with long range phase coherence. The transition is tuned with incremental depositions of normal metal Ag. Normal metal Ag affects the film in two ways. First, it suppresses the amplitude $\Delta(T)$ and T_{MF} by a proximity effect, and second, it improves the phase coupling. With Ag deposited instead of Pb to improve coupling, not only are phase fluctuations reduced, but the average order parameter amplitude is also reduced. The Ag does not immediately short the grains just as initial amounts of Pb on an insulating granular Pb film did not short the grains. The transport data show that the S-I transition can be broken into two regions where one region is dominated by phase fluctuations and the other region is dominated by amplitude suppression. Whenever phase fluctuations are reduced, the phase is stiffer.

The granular nature of quench condensed granular Pb films explored in chapter 4 naturally lends itself to probe variations of phase fluctuations and the effective film T_c. The film T_c is defined at the point where there is global phase coherence. Here superconductivity is supported. and the sheet resistance is zero below T_c. Normal metal Ag instead of Pb is deposited on top of an initial insulating granular Pb film to explore both improving coupling and the effect of suppressed T_{MF} on the film's T_c. In this manner. both phase fluctuations and amplitude variation can be explored in one morphology. The source of Cooper pairs is the Pb grains. and Ag provides an increased volume for them to roam in. [See figure 5.1]. Due to quasiparticles flowing into Pb from Ag, and Cooper pairs flowing from Pb into Ag. the energy gap is reduced. Normal metal Ag was chosen over other novel metals because it does not form an intermetallic compound with Pb and has no metalurgical solubility in Pb. Such metallurgical effects can interfere with simple models we are probing.

With the publication of the Emery-Kivelson theory [26] qualitatively describing doped high T_c superconductors, there has been increased interest in the connection between phase fluctuations and the critical temperature T_c of a superconducting material. The Emery-Kivelson theory of high temperature superconductors proposes the formation of Cooper pairs below a BCS mean field temperature T_{MF} but no global phase coherence until a lower temperature T_c. In a conventional bulk superconductor, the film T_c and the mean field temperature T_{MF} occur nearly simultaneously. With strong phase fluctuations, however, global phase coherence is destroyed. and so a temperature, T_θ^{max}, is defined in the Emery-Kivelson theory to represent the temperature above which phase fluctuations destroy global phase coherence. Small regions of superconductivity can exist below T_{MF} but without global phase coherence until below T_θ^{max}. This is analogous to two dimensional quench condensed granular films we study here.

The coupling energy of Cooper pairs gives a measure of how well Cooper pairs are coupled to each other in the superconducting condensate. To remove a Cooper pair from a phase coherent condensate and place it into another phase coherent

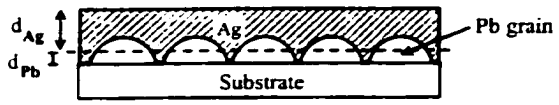

Figure 5.1: Cartoon showing morphology of granular Pb/Ag film.

The mean thickness of Pb and Ag evaporated corresponds to d_{Pb} and d_{Ag} respectively.

condensate of a different phase without breaking the Cooper pair takes some minimum binding energy, E_b. Within a volume of some phase coherence, a larger E_b is resistant to thermal fluctuations and keeps Cooper pairs bound to the same phase coherent condensate. But phase fluctuations can occur between local regions if the overlap of each region's superconducting wavefunction is not strong enough to bind both regions to a common phase. To suppress phase fluctuations between local regions requires the rapid movement of Cooper pairs between local volumes to maintain a high uncertainty in ΔN. According to the particle-phase uncertainty relation described in chapter 2, this will ensure a well defined phase ϕ common to both regions. The "Ag bridging" allows rapid Cooper pair flow between adjacent superconducting grains of varying phase. Thus normal metal Ag can improve grain coupling while a proximity effect suppresses the energy gap, or order parameter amplitude. With a proximity effect, the density of Cooper pairs is reduced, and hence, superconductivity is reduced to a lower T_c.

5.2 Results

The experimental procedure to examine quench condensed granular Pb/Ag films is very similar to that used for quench condensed granular Pb films. The main differences were in using a simple insert stick instead of a He3/He4 dilution refrigerator because the refrigerator had ceased functioning, and instead of a single

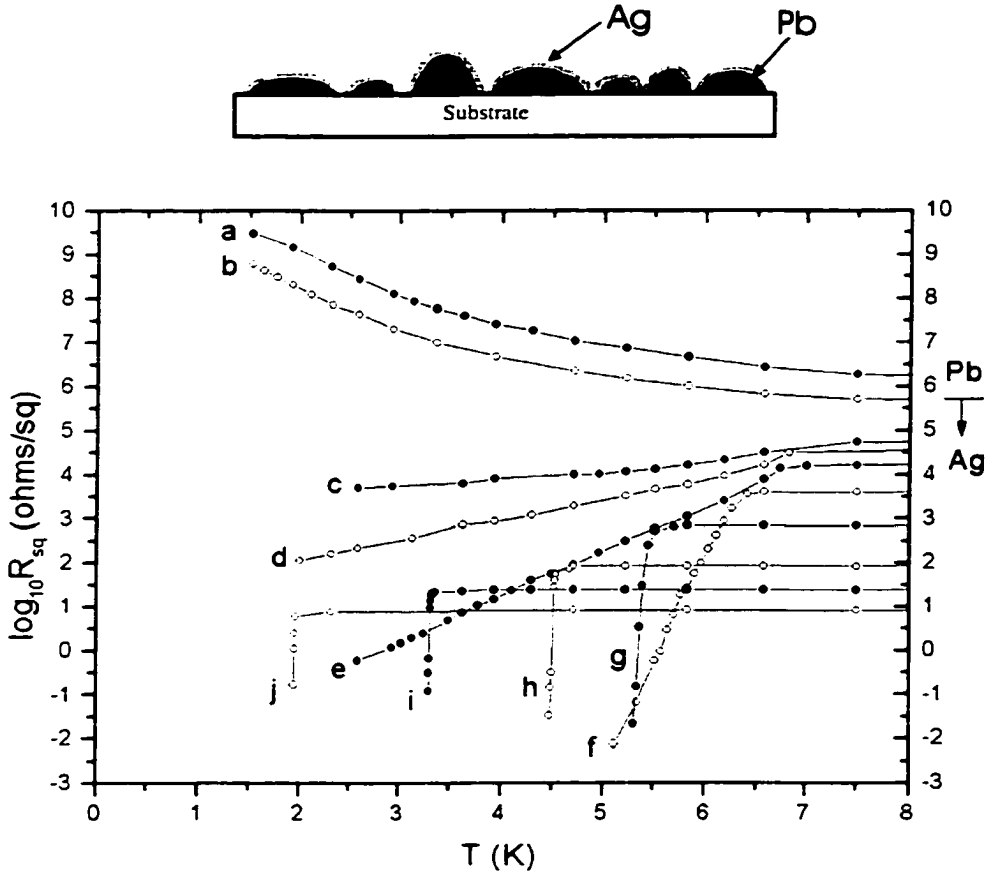

Figure 5.2: Transport of a granular Pb/Ag film with an initial insulating granular Pb film

Initial granular Pb film has insulating transport. Sheet resistance transport of a quench condensed granular Pb film followed by Ag depositions. The initial Pb film is in the strongly localized regime and is approximately 100 Angstroms thick.

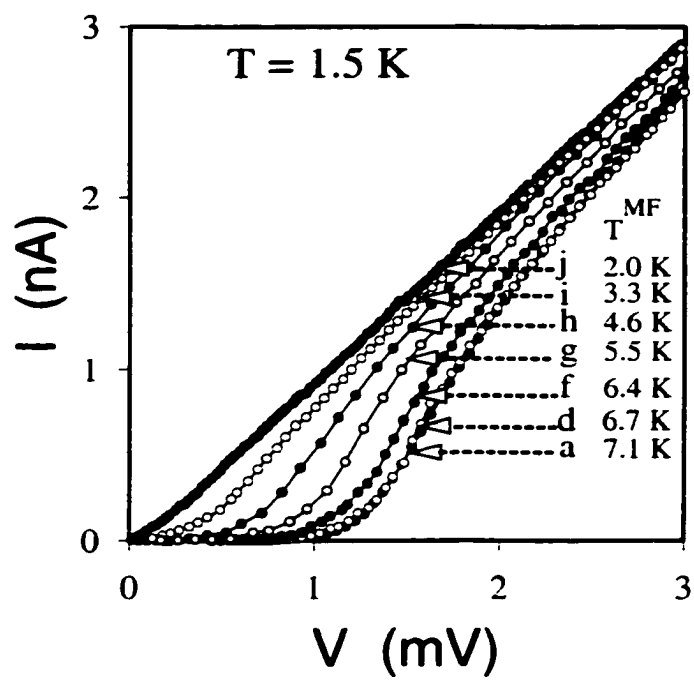

Figure 5.3: Tunnel I-V plots of a granular Pb/Ag film at 1.5 K

The tunnel junction probes the BCS mean-field transition temperature, T_{MF}. The letters refer to the corresponding transport plots in the previous figure.

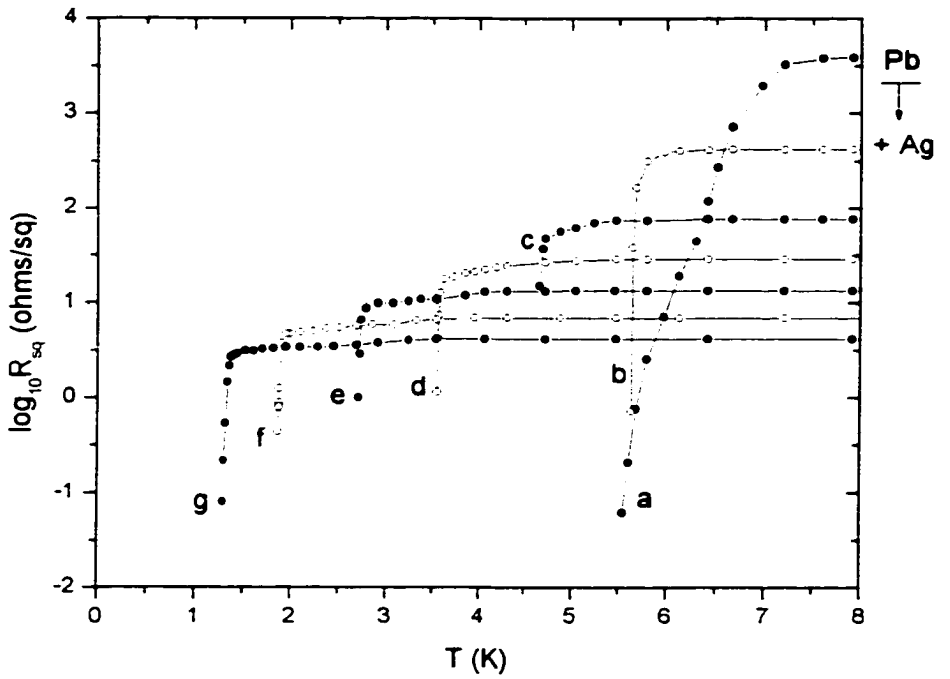

Figure 5.4: Transport of a granular Pb/Ag film with an initial superconducting granular Pb film

Initial granular Pb film has superconducting transport. Sheet resistance transport of a quench condensed granular Pb film followed by Ag depositions.

source of Pb, another source of Ag is added. The same substrate configuration is used as that described in chapter 3 to allow simultaneous transport and tunneling measurements.

In most experiments, we began with an initially insulating granular Pb film of about 100 Angstroms mean thickness as the base layer for incremental depositions of normal metal Ag. For comparison, measurements were also taken with an initial Pb film with superconducting transport and a slightly wide resistive transiton. Four-point transport measurements as a function of temperature were converted to R per square and are plotted on a log R vs T. The transport for an initially insulating granular Pb film followed by Ag is shown in figure 5.2. Curve a is an initial granular Pb film with insulating transport deposited onto a substrate held at 10 K. With only a few Angstroms of Ag deposited, the film crosses through the S-I transition. Curves b-f resemble the transport of a quench condensed granular Pb film in that the S-I transition occurs at about 10^5 ohms and there are long resistive tails in the weakly localized region. T_{MF} is suppressed from 7.1 K to 6.5 K in plots c-f as depositions of normal metal Ag increase coupling of Pb grains. Curves g-j in the extended region of global phase coherence require larger incremental depositions of Ag to reduce the normal state sheet resistance, and this further depresses T_{MF} of the film to 2 K at $R_n = 10$ ohms. This behavior contrasts that of a pure granular Pb film at 10 ohms, where the film T_c is at 7.2 K, the bulk value of Pb.

With a base electrode of Al-Mn and an oxide barrier, tunneling measurements were made on the Pb/Ag films in an analogous method to that of Pb films in the previous chapter. The results are shown in figure 5.3. Normal metal Ag couples groups of superconducting Pb grains such that a larger area of phase coherence exists, but the average superconducting order parameter amplitude is reduced due to the proximity effect. Curves a-f do not change too much from the bulk BCS tunneling I-V of Pb, but for curves g-j, the superconducting energy gap decreases as more normal metal Ag is added. This directly illustrates the proximity effect of Ag: a reduction in both the T_{MF} and superconducting energy gap of the film. The

tunneling data directly probes the superconductivity of the film on a local scale.

For comparison, a base granular Pb film with superconducting transport and a slightly wide transition is used instead of an insulating base granular Pb film. Normal metal Ag is then incrementally deposited on top. The transport is seen in figure 5.4. Notice that the T_c is suppressed as more Ag is added, and the transitions are very sharp. The broad resistive transitions of figure 5.2 are not found in this plot.

5.3 Proximity Effect

In figure 5.5, the low temperature energy gap is plotted versus the T_c for both a uniform Pb film and two granular Pb/Ag films. Using a simplex fitting algorithm described in chapter 4, the superconducting energy gap Δ was found for a variety of Ag thicknesses on granular Pb. The energy gap at T=0, Δ_0, was found using a plot of the BCS energy gap as a function of temperature [27]. With a known T, T_c, and $\Delta(T)$, a Δ_0 at T=0 can be found using this plot. As stated before, T_{MF} was taken as the value at half the normal state sheet resistance. In a uniform Pb film, the suppressed T_{MF} and Δ correspond with a suppressed density of quasiparticle states, N(0), characteristic of a thin disordered film. In Pb/Ag films, the suppressed T_{MF} and Δ correspond with a suppressed superfluid density characteristic of a proximity effect. With a normal metal next to a superconductor, the sea of Cooper pairs becomes diluted as it expands to fill a larger volume. The number of pairs is the same but the density of overlap is less. As more Ag is deposited, the film thickness increases, and T_{MF} and Δ decrease. The uniform Pb film and the Pb/Ag film follow approximately the same linear relation between T_{MF} and Δ. As seen in figure 5.5, for the same amplitude, the Pb/Ag film has a larger T_{MF} than a uniform film. In the BCS relation of coupling, T_c is used in the denominator where T_c refers to T_{MF} and not the film T_c unless they occur simultaneously. In the case of bulk superconductors and uniform films, film T_c and T_{MF} occur nearly simultaneously, but in granular films, they do not.

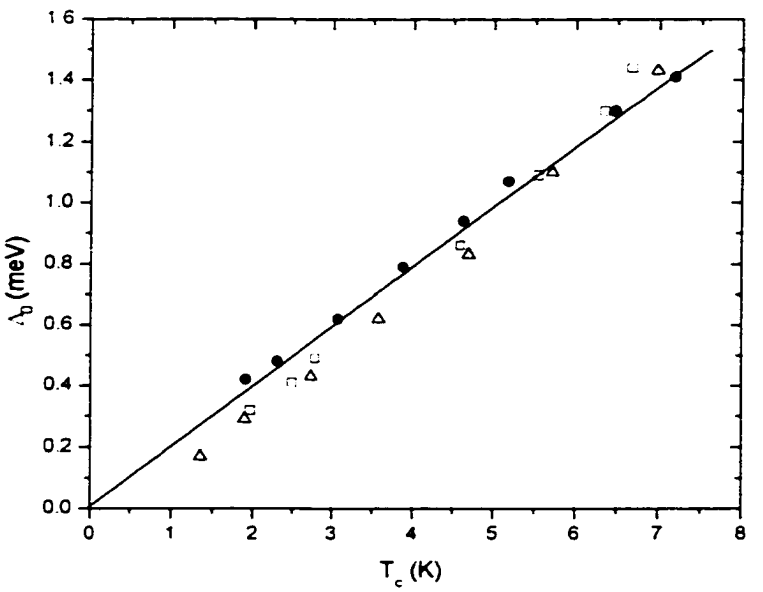

Figure 5.5: Energy gap at T=0 and corresponding T_c for various film thicknesses in uniform Pb films and granular Pb/Ag films.

The filled circles are for a uniform Pb film, the open squares are for a base granular Pb film with insulating transport followed by Ag depositions , and the open triangles are for a base granular Pb film with superconducting transport followed by Ag depositions.

When the temperature is lowered below T_{MF}, Cooper pairs correlate in some coherence volume. Quasiparticles from normal metal Ag flow into Pb and Cooper pairs from Pb flow into Ag. Proximity theory from chapter 2 predicts that N(0)V is continuously changed as the fraction of Ag to Pb changes. This results in an exponential dependence of the energy gap Δ on fractional thickness. In the Cooper theory of the proximity effect, one would use the total volume of Pb+Ag in equation 2.24 to modify the product $N(0)V$. In the product of N(0)V, V is the interaction potential between two electrons in a Cooper pair. From the equation $\Delta = 2\hbar\omega_D e^{-1/N(0)V}$, N(0)V changes and this results in a corresponding change of Δ. In the deGennes theory of the proximity effect, a more sophisticated formula, equation 2.25 is used. These formulas apply in the Cooper limit where the coherence length is larger than the film thickness. A plot using the simple Cooper theory is shown in figure 5.6 for Pb with $N(0)V$=0.39 and a Debye temperature of 96 K [28].

The data shown in figure 5.7 suggests the Ag increases the volume that Cooper pairs can extend in, and this reduces the Cooper pair density. The lines are a guide to the eye in figure 5.7. The N(0)V value is initially changed as Ag is added to an insulating film of granular Pb as one would expect for a proximity effect and the energy gap is correspondingly decreased from the bulk value of Pb. The value of Δ does not appear to decrease as an exponential dependence on fractional Ag thickness as shown in figure 5.6, but rather according to a volume dilution of Cooper pairs. If the coupling value, $2\Delta/kT_c$ stayed constant, T_{MF} should follow the linear dependence of Δ with increasing volume fraction of Ag. But T_{MF} is enhanced above this expected value.

5.4 Emery-Kivelson Theory

The Emery-Kivelson theory [26] examines phase stiffness in high T_c superconductors. Phase stiffness refers to the susceptibility for phase fluctuations and it is of interest here because the ideas can be quantitatively applied to granular Pb/Ag

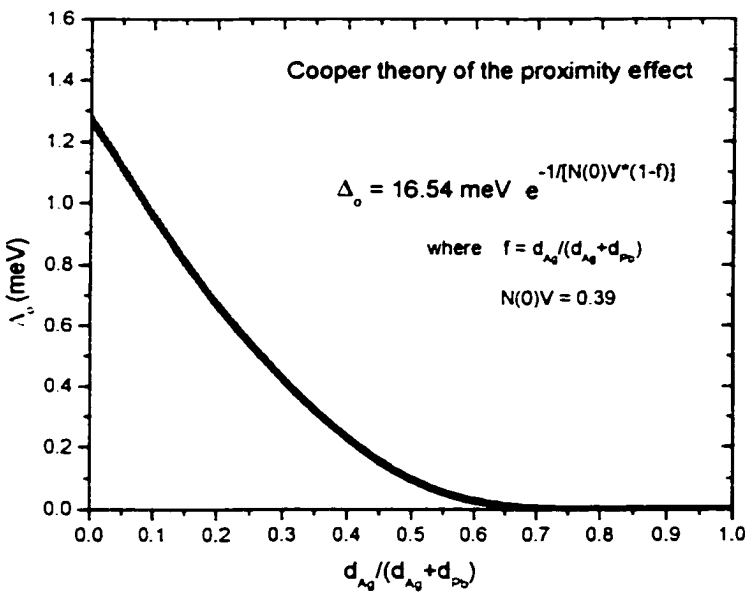

Figure 5.6: Cooper theory of the proximity effect

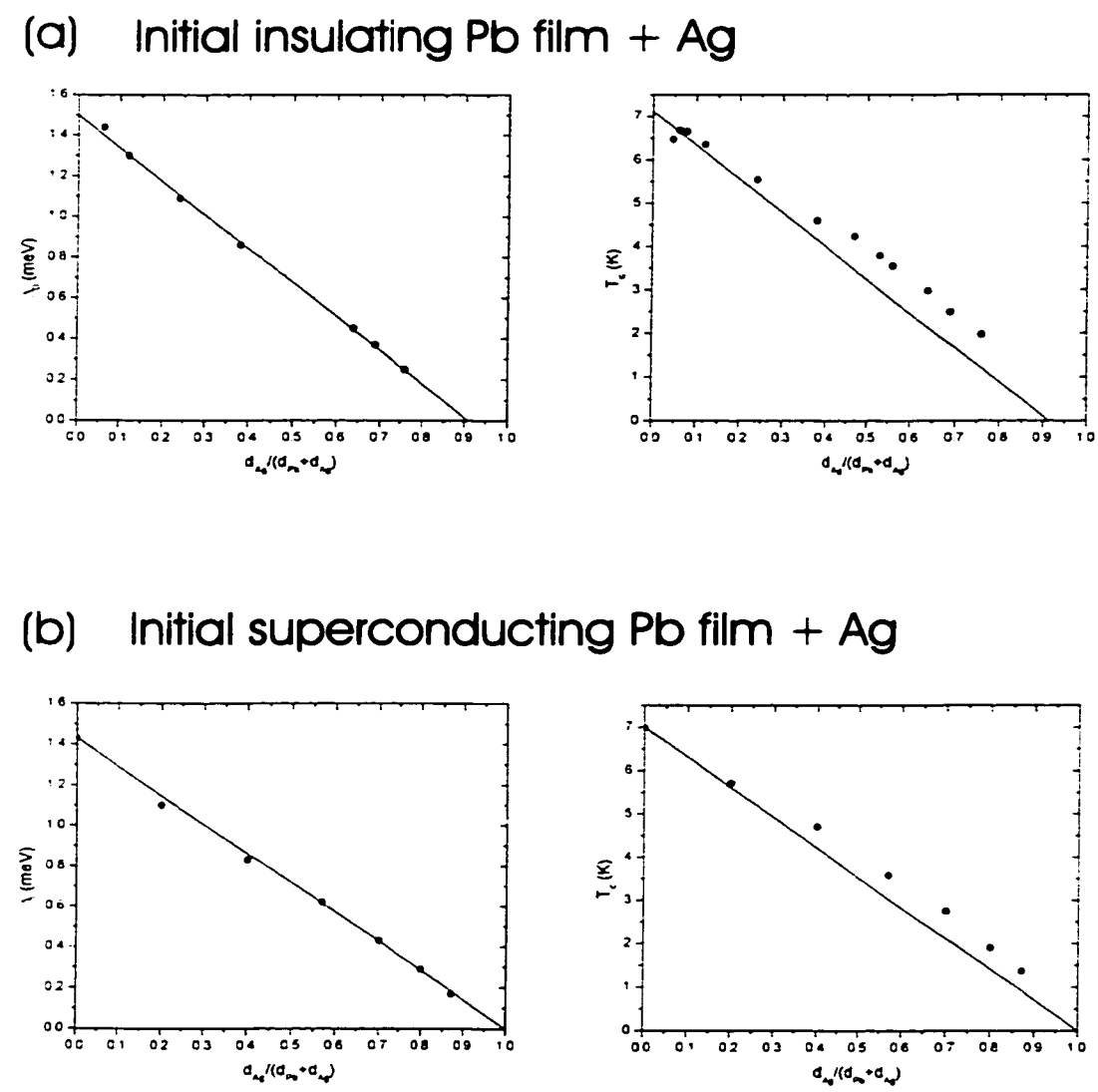

Figure 5.7: Effect of fractional Ag thickness on Δ_0 and T_c

Energy gap at T=0, Δ_0, and transition temperature evaluated at half the normal state sheet resistance, T_c, are plotted versus fractional thickness of Ag. The lines are a guide to the eye.

films. Superconductivity results from overlapping Cooper pair wavefunctions that fit into each other with a common phase. The denser the wavefunctions that fit into each other, the lower the system energy and the larger the energy gap Δ is. This stiffness against phase fluctuations can be represented by some characteristic temperature called T_θ^{max}. If the thermal energy, kT, is larger than T_θ^{max}, the thermal energy is enough to result in phase slippage. The temperature below which Cooper pairs form is the BCS mean-field temperature, T^{MF}. The possibility of two different temperatures imply that locally, there can be a region of phase coherent Cooper pairs below T_{MF}, but globally, phase fluctuations destroy any long range phase coherence above T_θ^{max}. The film T_c with global phase coherence therefore is bounded by both T_θ^{max} and T^{MF}. If $T_\theta^{max} < T_{MF}$, phase fluctuations dominate and T_c occurs below T_θ^{max}. If $T_\theta^{max} > T_{MF}$, amplitude suppression dominates and T_c occurs below T_{MF}. This phase diagram can be seen in figure 5.8.

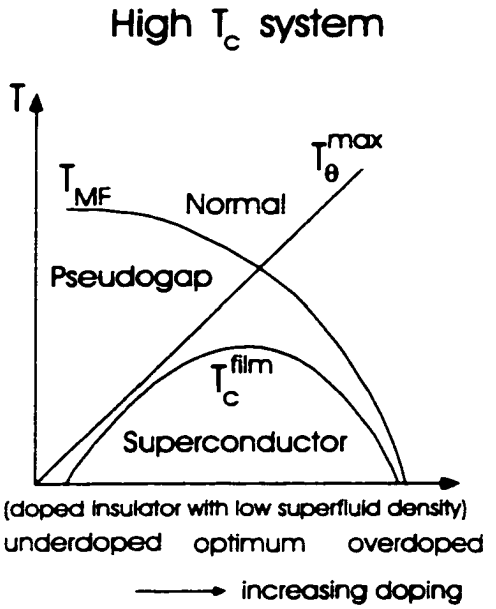

Figure 5.8: Phase diagram of Emery-Kivelson theory for doped high T_c superconductors.

Emery and Kivelson emphasize that the reason phase fluctuations are so im-

portant is because the oxide superconductors are doped insulators with a very low superfluid density. Emery and Kivelson postulate that this low superfluid density results in a susceptibility to phase fluctuations which then can destroy long range superconductivity. High temperature superconductors such as YBCO are superconducting in two dimensional planes weakly coupled to each other. See reference [29] for more infomation and references therin. There are phase-fluctuations in-plane and between planes in high T_c superconductors.

The variation of T_θ^{max}/T_c is used as a guide to phase fluctuation importance in underdoped, optimally-doped, and overdoped high temperature superconductors. A simple model phase diagram is seen in figure 5.8. In the underdoped region of the phase diagram between T^{MF} and T_θ^{max}, there are still local regions of superconductivity and hence an energy gap (as in the insulating Pb case) referred to as a pseudogap. A pseudogap is a suppression in the density of states at low energy: experimentally it is not a BCS "full" gap in which low energy quasiparticle states are completely suppressed at T=0. This is interesting because the pseudogap appears at a temperature larger than the measured critical temperature, T_c, of the superconducting film, indicating the possible existence of Cooper pairs but not enough overlap of Cooper pairs to resist phase fluctuations and form a globally phase coherent superconducting state.

5.5 Discussion

A granular Pb/Ag film has sheet resistance properties that depend both on phase fluctuations and amplitude suppression. This is clearly seen in the sheet resistance transport plot of figure 5.9 where phase fluctuations lead to long resistive tails, and amplitude suppression leads to suppressed T_{MF}. It is instructive to compare the transport of a Pb/Ag film to that of a granular Pb film in which phase fluctuations are important and to that of a uniform Pb film in which amplitude suppression is important. This comparison is shown in figure 5.9.

In figure 5.9a, the transport curves b-f of granular Pb plus Ag are compared with

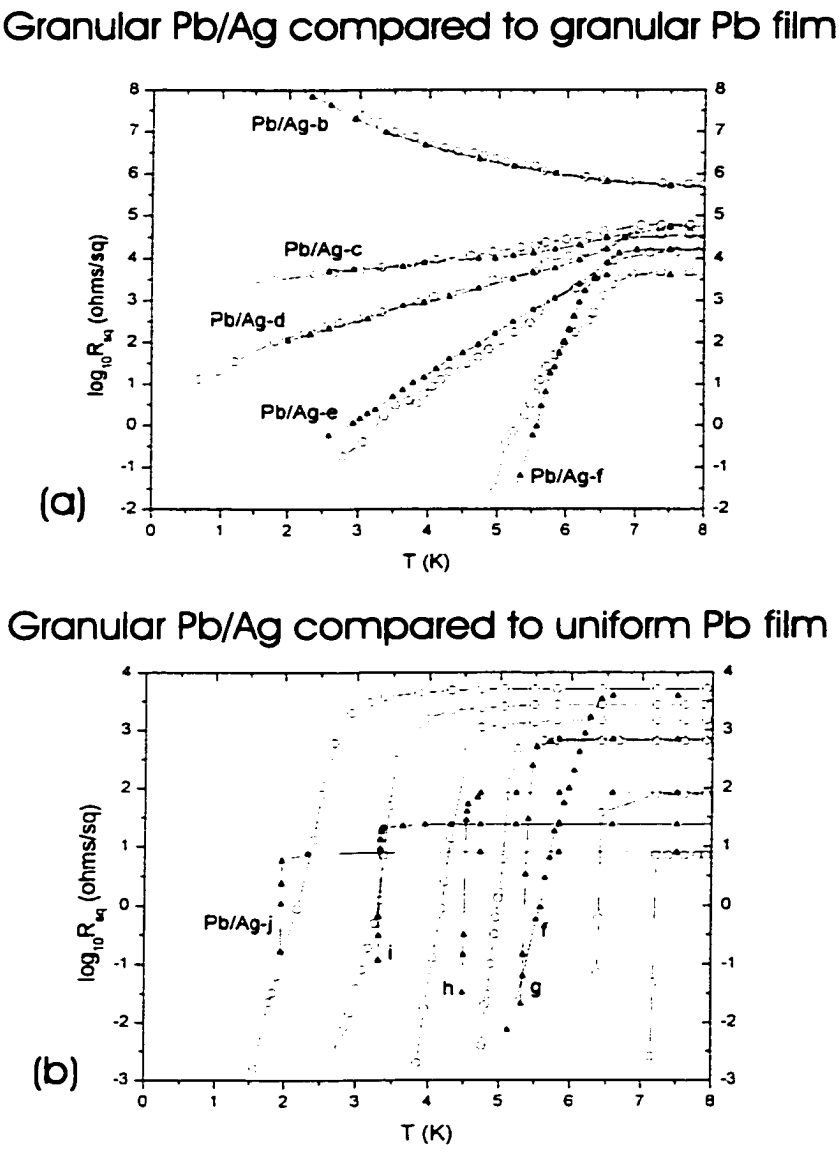

Figure 5.9: Transport of Pb/Ag system compared to transport of granular Pb system and uniform Pb system

(a) Sheet resistance transport of granular Pb/Ag film compared to granular Pb film. (b) Sheet resistance transport of granular Pb/Ag film compared to uniform Pb film. Solid triangles are Pb/Ag and open circles are Pb.

transport curves of granular Pb at similar values of normal state sheet resistance. For plots b-e, T_{MF} calculated at half the normal state sheet resistance is near 7 K and the slopes of the long resistive tails are nearly the same as those of granular Pb. This indicates that the normal state sheet resistance is a determining factor of the slope of a resistive tail. It is the number of phase slips due to phase fluctuations and thermal energy that determines the sheet resistance along a resistive tail. In both granular Pb/Ag films and granular Pb films, the transport is dependent on a random two dimensional array of Josephson junctions that vary in coupling strength. In a granular Pb film, only additional Pb is used to improve coupling. In the case of a Pb/Ag system, Ag is used to improve coupling. The proximity effect enables Ag to approximate the effect of Pb with the added effect of ultimately reducing T_{MF}. Notice that curve f of the Pb/Ag film has a sharper slope than the corresponding granular Pb film normal state sheet resistance curve. Curve f also has a markedly reduced T_{MF} from those of curves c, d, and e.

In figure 5.9b, a granular Pb/Ag film is compared with a uniform Pb film at approximately the same normal state sheet resistance values. Notice the sharper transition for Pb/Ag films and the similarities with a uniform film for the transport plots where the T_{MF} is reduced. In particular, curve f has a higher T_{MF} than the corresponding uniform film at the same normal state sheet resistance. The slope of curve f is about the same as that of the uniform film. Curve g of the Pb/Ag film also has a larger T_{MF} at the same normal state sheet resistance as a uniform film, but in this case, the slope of curve g is sharper than that of the uniform film. Plots h,i, and j of the Pb/Ag film all have sharp transitions as does the uniform film at these normal state sheet resistance values, but the difference is that T_{MF} continues to increase in a uniform film.

The similarities between the Emery-Kivelson phase diagram of a high T_c superconductor system and a granular Pb/Ag system are remarkable. A cartoon of the Emery-Kivelson phase diagrams of the two systems is shown in figure 5.10. The major difference between these phase diagrams is the appearance of a pseudogap in a high T_c system on the underdoped side, and the appearance of a full BCS

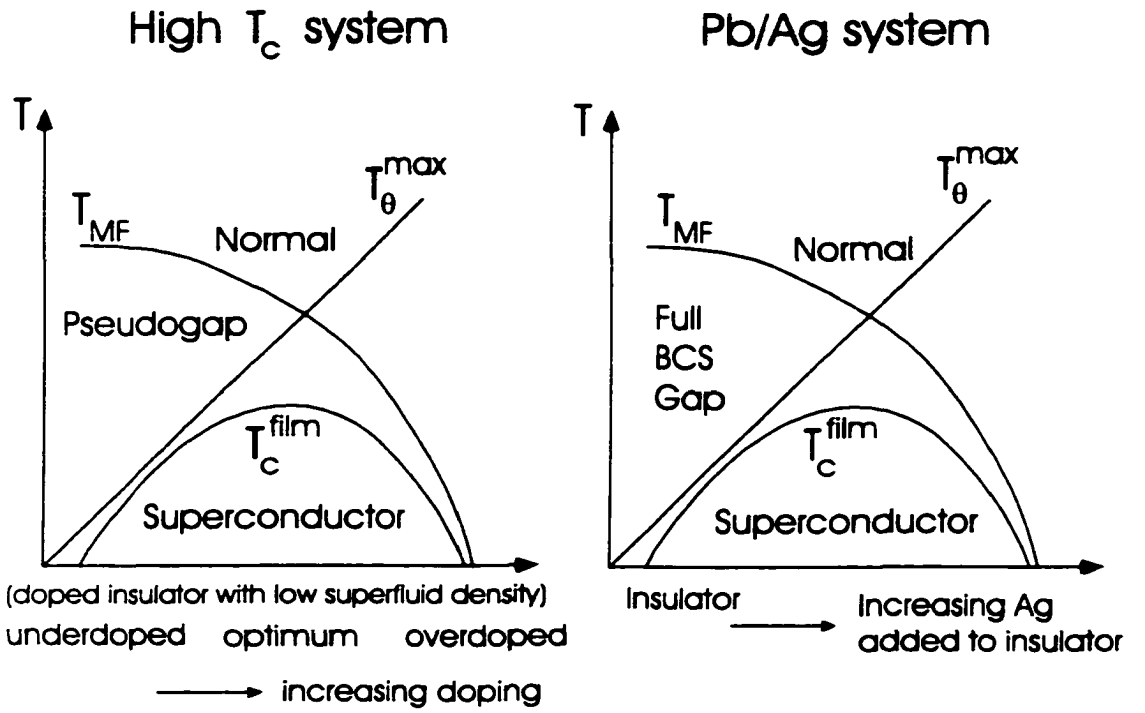

Figure 5.10: Comparison between Emery-Kivelson phase diagram of a low T_c granular Pb/Ag film and a high T_c film.

gap in a Pb/Ag system. Both the pseudogap and the BCS gap appear above the measured T_c and below T_{MF}. Thus, in both systems, Cooper pairs have formed and begun to condense in such a way as to lower the system energy and reduce the quasiparticle density of states at low voltage bias. The pseudogap in an underdoped high T_c superconductor implies that for a low applied voltage across a tunnel junction measuring the density of states, quasiparticles forming Cooper pairs are easily broken from the condensate. In other words, the quasiparticles are not strongly bound to the condensate. In a low T_c superconductor, the quasiparticles forming Cooper pairs are normally strongly bound to the condensate and not easily broken with an applied voltage across the tunnel junction. The tunneling density of states clearly shows a suppressed current until an applied voltage near the energy gap in a low T_c superconductor. The Cooper pairs in an underdoped high T_c superconductor are not strongly coupled at all, and thus the phase stiffness parameter, T_θ^{max} is very small. In a granular Pb/Ag film, the coupling of Cooper pairs at low Ag deposition is still very strong and near the BCS value. The phase stiffness parameter, T_θ^{max} is small, however, because of the granular morphology and the weak coupling between grains.

From the Emery-Kivelson phase diagram of figure 5.10, it is seen that the global phase coherent state of the film does not occur until below T_c. On the left of the phase diagram, the film T_c is bounded more by the phase stiffness temperature T_θ^{max}. Here, phase fluctuations are critical in limiting global phase coherence. On the right of the phase diagram, the film T_c is bounded more by the BCS mean-field temperature T_{MF}. Global phase coherence and the formation of Cooper pairs are nearly simultaneous in this region. These limits on film T_c with global phase coherence in the Emery-Kivelson theory are very similar to the limits on global phase coherence in a Pb/Ag system.

In a high T_c system, holes act as a doping agent to an initial underdoped high T_c superconductor. Emery-Kivelson envision an inhomogeneous material, much like the Pb/Ag system, and Josephson coupling across these regions. The holes are what form the pairs. In the Pb/Ag system, the grains are superconducting

and connected via Josephson coupling. Holes doped into an underdoped high T_c system form more pairs per unit volume. Ag "doped" into an initially insulating granular Pb system decreases the number of pairs per unit volume. Increasing the number of holes in an underdoped high T_c system improves Josephson coupling, and increasing the amount of Ag in a Pb/Ag system improves Josephson coupling. For reasons not yet understood, the increased doping of holes in a high T_c system suppresses T_{MF}, and hence, the film T_c is also suppressed. Due to a proximity effect, increased doping of Ag in an insulating granular Pb film suppresses T_{MF}, and hence the film T_c is also suppressed. The temperature T_θ^{max} is increased in both the high T_c system and the Pb/Ag system by decreasing phase fluctuations via increasing the Cooper pair transfer rate between local superconducting regions in the system. This is due to the uncertainty relation between particle number N and phase ϕ discussed in chapter 2. The Cooper pair transfer rate is increased by doping holes into an underdoped high T_c system and improving Josephson coupling by increasing the number of pairs, and by "doping" Ag into an insulating granular Pb system and improving Josephson coupling by improving quasiparticle conduction.

To illustrate the connection between Pb/Ag transport and the underdoped side of the Emery-Kivelson phase diagram where phase fluctuations dominate, figure 5.11a is an attempt to show where transport in a Pb/Ag system would fall on an Emery-Kivelson phase diagram. For the transport curves a-f, phase fluctuations are the determining factor of the resistive tails. This can be seen by the wide transitions all occurring below a T_{MF} of approximately 7 K. The base film was an insulating granular Pb film. Further depositions of normal metal Ag drive it through the S-I transition. Plot f is more clearly headed toward global phase coherence and zero resistance than plots c-e. The temperature at which plot f will have a zero resistance is referred to as the film T_c and is lower than T_{MF} calculated at half the normal state sheet resistance. It's then presumed that plots c-e will also have some film T_c lower than T_{MF} if the plots do indeed go to zero resistance. We can identify a value for T_c, and it is increasing as the normal state

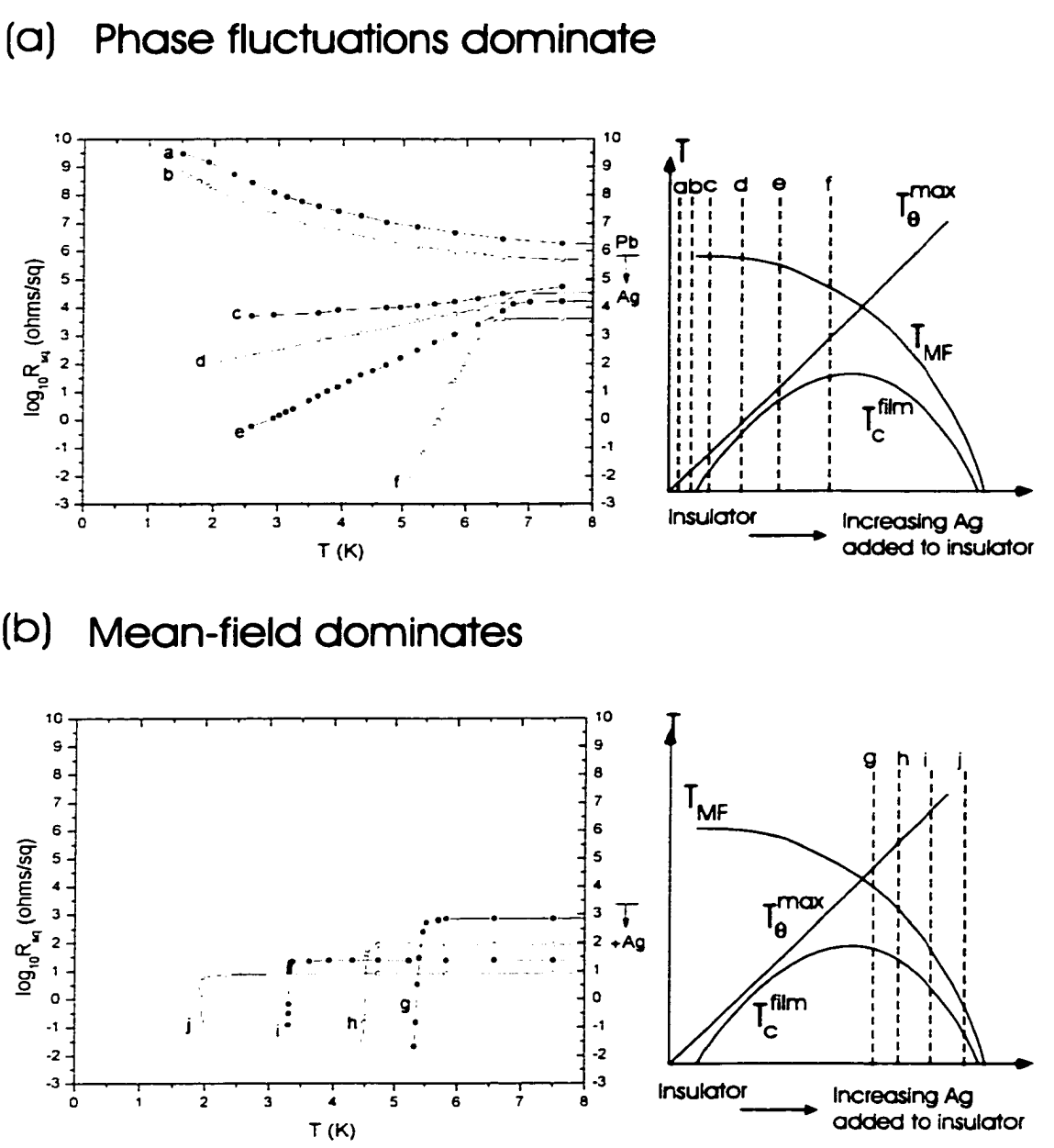

Figure 5.11: Comparison of granular Pb/Ag system with Emery-Kivelson phase diagram

(a) Transport curves a-f for granular Pb/Ag film showing influence of phase fluctuations. (b) Transport curves g-j for granular Pb/Ag film showing influence of amplitude suppression. The dashed lines are a guide to the eye.

sheet resistance decreases due to increasing depositions of Ag. At the same time, T_{MF} is decreasing, but it is higher than the film T_c. This is analogous to the left side of the Emery-Kivelson plot where phase fluctuations dominate the mean-field T_c in determining the film T_c. So local superconductivity exists, but not global superconductivity.

On the overdoped side of the Emery-Kivelson phase diagram transition, mean field temperature dominates the film T_c. Figure 5.11b illustrates this with a cartoon showing where the transport of a Pb/Ag system would fall on the phase diagram. For the transport curves g-j, the resistive transitions are sharp, and the film T_c occurs at T_{MF} which is suppressed from the bulk value due to amplitude suppression. Increasing depositions of normal metal continue to improve conductivity, but phase fluctuations are no longer important in the temperature range below T_{MF}. Due to additional depositions of Ag, T_{MF} is suppressed via a proximity effect.

5.6 Conclusions

Normal metal Ag allows both the amplitude and the coupling of superconducting order parameters to be varied. In doing so, an analogy is found to a high T_c system with a phase diagram proposed by Emery and Kivelson. A division in the transport is seen between coupling strength and phase fluctuations and amplitude and mean-field temperature suppression.

Chapter 6

Quench condensed granular Pb film followed by a few monolayers of Sb and then Pb or Ag

6.1 Introduction

In this chapter, we examine a combination of granular and uniform morphologies to probe the superconducting order parameter through an S-I transition. As we have already shown, phase fluctuations are important in granular films, and amplitude fluctuations are important in uniform films. Here we study a combination of phase fluctuations and amplitude suppression. In chapter 5, phase fluctuations and amplitude suppression were also studied via a proximity effect of Ag directly next to Pb. In this chapter, an Sb layer separates Pb and Ag. The case of Pb deposited onto the Sb layer instead of Ag is used for comparison. An initial quench condensed granular Pb film of 25 Angstroms mean thickness was deposited on a glass substrate. This film was granular and consequently not electrically continuous. From previous experiments on uniform films, it is known that a few monolayers of Sb on a substrate followed by a few monolayers of Pb will result in a disordered uniform film with electrical continuity. For this experiment,

we evaporate a few monolayers of Sb over the initial granular Pb film in the hope that evaporating Pb on top of this Sb would result in a uniform film. However, instead of 5-10 Angstroms of Pb needed on top of Sb on a substrate of glass, 25 Angstroms of Pb was required before electrical continuity was achieved. Thus the amount of Pb needed for electrical continuity lies between the value needed for a uniform film, 5-10 Angstroms, and the value needed for a granular film, 90-100 Angstroms.

A possible explanation for this discrepancy is that the dangling bonds of Sb were partially saturated by the underlayer of Pb. In former experiments on uniform Pb, Sb was directly deposited onto an insulating substrate of glass. Perhaps in some area about each Pb grain, the Sb is saturated by roaming electrons as shown in figure 6.1 a,b, and c. Then these saturated bonds are not available to bind subsequently evaporated Pb atoms and a granular morphology can form on top of this saturated area. Some regions are not saturated, however, and can bind Pb atoms to form a uniform morphology. So the top layer of Pb over the Sb underlayer could be a combination of granular and uniform morphology as shown in figure 6.1d. The Pb grains are superconducting at a higher temperature than a uniform film at the same normal state sheet resistance. So the uniform film acts as a quasiparticle bridge between superconducting Pb grains.

The transport plots show a combination of uniform behavior and granular behavior. Both phase fluctuations and amplitude supression contribute to the modification of the superconducting order parameter. The film T_c in both systems is suppressed from the bulk T_c of Pb, with greater suppression in the Pb-Sb-Ag film due to the proximity effect of Ag. Tunneling measurements were taken only on the Pb-Sb-Ag film.

This experiment was performed with the simple insert stick described in chapter 3. The substrate condfiguration and experimental methods are the same as described in chapter 3. Sources of Pb and Sb were used to deposit the Pb-Sb-Pb film, and sources of Pb, Sb, and Ag were used to deposit the Pb-Sb-Ag film. The sample configuration is identical to that described in chapter 3.

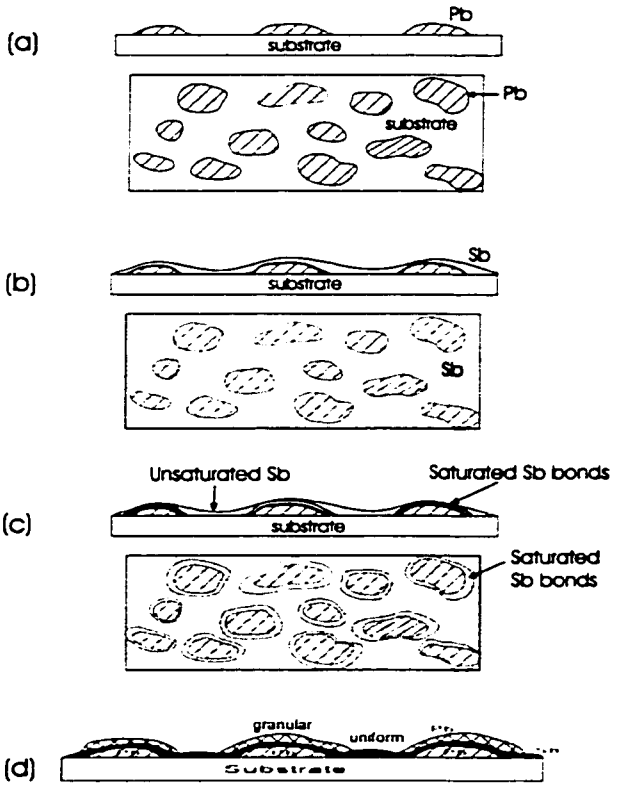

Figure 6.1: Cartoon of Pb-Sb-Pb/Ag morphology

(a) An initial film of granular Pb is deposited with no electrical continuity. The mean thickness of the Pb is 25 Angstroms. (b) A few monolayers of Sb is deposited on top of these grains and the glass substrate. The mean thickness of the Sb is 20 Angstroms. (c) The Sb possibly saturates its bonds in the vicinity of the Pb grains. The regions of Sb over glass do not saturate their bonds. The region of saturated bonds of Sb possibly resembles that of a neutral glass substrate. The region of unsaturated bonds of Sb on glass act as a few monolayers of Ge would in a uniform Pb film by binding to Pb atoms as they fall. There is no electrical continuity yet. (d) Further depositions of Pb achieve electrical continuity with a mean thickness of 25 Angstroms. It's possible that this Pb from the deposition forms grains on top of the saturated bonds of Sb and forms a uniform film on top of the unsaturated bonds of Sb. The Pb atoms from the deposition source could be more attracted to Pb grains composed of clumping Pb atoms than the uniform Pb film composed of a base layer of Pb atoms bound to unsaturated Sb. Thus, the final morphology is a film of Pb grains surrounded by a uniform Pb film, and all of this on top of a layer of Sb.

6.2 Results

Transport measurements are plotted on a log R vs T plot since the sheet resistance varied over 10 orders of magnitude. The transport measurements for both the Pb-Sb-Pb film and the Pb-Sb-Ag film are plotted in figure 6.2. A base temperature of 1.7 K could be reached using the simple insert stick. Thus it is not clear from the transport plots whether many of the curves will tend toward insulating or superconducting behavior. In both systems, the transport resembles granular transport because the resistive tails fan out from approximately the same T_{MF}. It's interesting that the Pb-Sb-Pb film has a suppressed T_{MF} from that of 7.1 K seen in granular Pb films. T_{MF} could be suppressed in Pb-Sb-Pb films due to the high density of localized states in the Sb, which enables Cooper pairs to extend into the Sb and a proximity effect to take place. As would be expected, T_{MF} is suppressed in the Pb-Sb-Ag films due to the proximity effect of normal metal Ag. As more Pb is added in the Pb-Sb-Pb films, T_{MF} increases. As more Ag is added in the Pb-Sb-Ag films, T_{MF} decreases.

The insulating transport is very similar to a uniform Pb film in that both exhibit insulating behavior at low temperatures at similar normal state sheet resistances. of a uniform film since the grains are not Josephson coupled. In the morphology picture for a Pb-Sb-Pb film, the layer on top of the Sb film consists of physically separated grains sitting in a sea of a uniform film. If the grains are superconducting, but the normal state sheet resistance is not low enough for the uniform film to superconduct, transport is entirely due to quasiparticles traversing the system via the uniform film interspersed between the grains. Until a supercurrent channel between the superconducting grains exists, the current is likely to pass only through the uniform film. The grains act as physically separated superconductors where the uniform film acts as the barrier between them. As the conduction of the uniform film improves, the chances of a Cooper pair channel forming also improve. A proximity effect of the superconducting Pb grains near a normal uniform film can lead to some area of uniform film superconducting around each grain. This

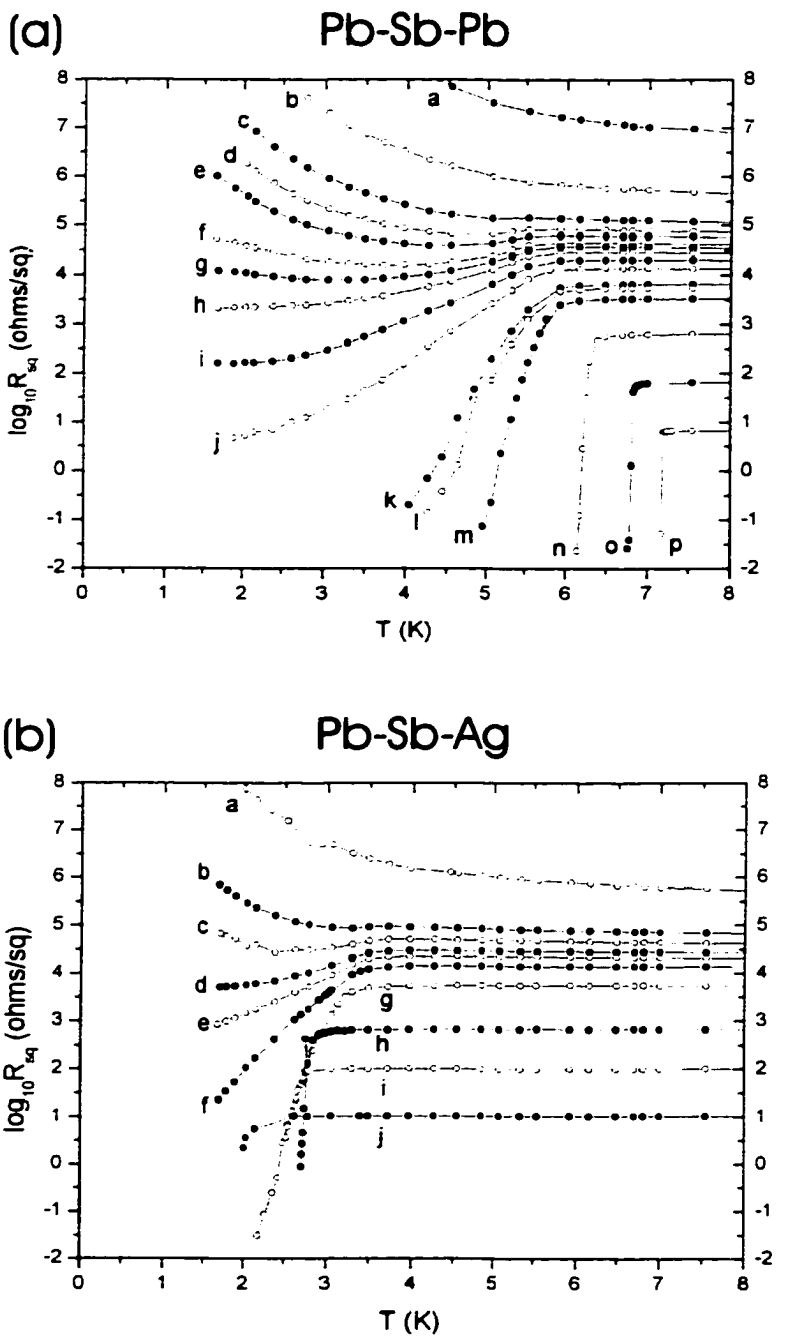

Figure 6.2: Transport for a Pb-Sb-Pb film and a Pb-Sb-Ag film

(a): 25 Angstroms Pb + Sb + Pb (b): 25 Angstroms Pb + Sb + Ag

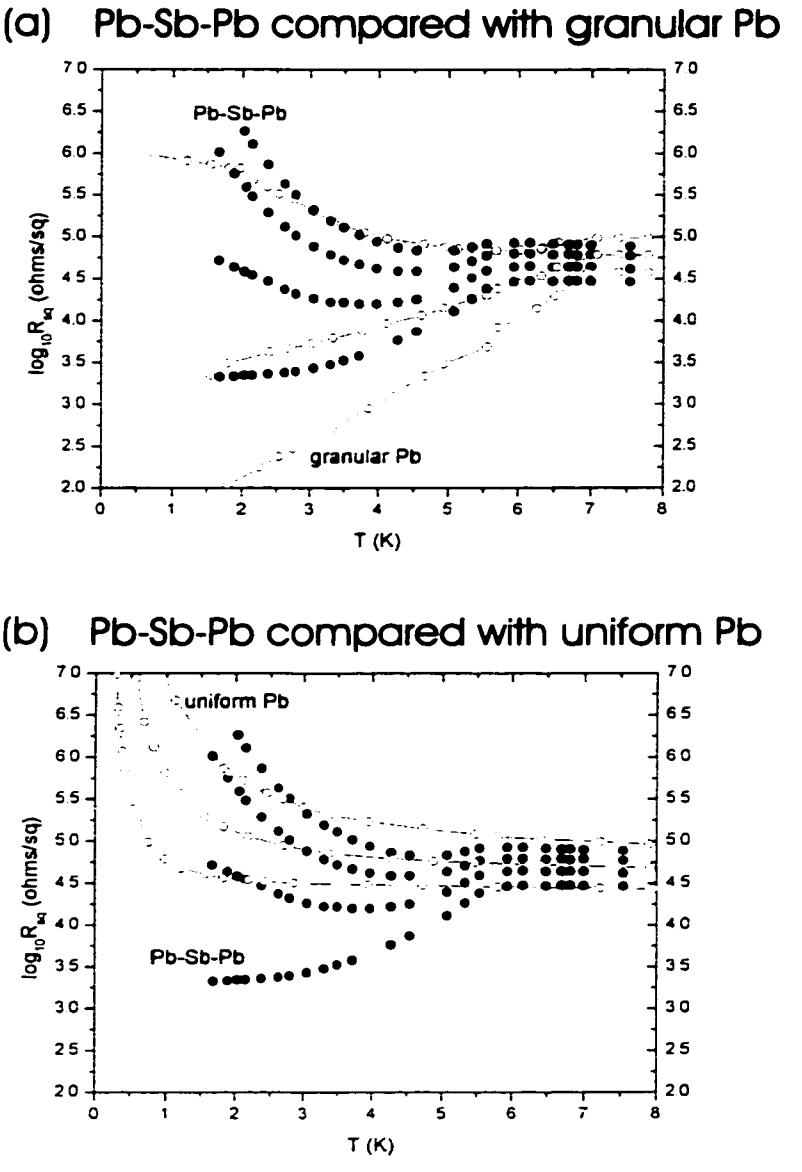

Figure 6.3: Quasi-reintrant transport of Pb-Sb-Pb film

Pb-Sb-Pb film quasi-reintrant transport compared to transport of a granular Pb film in (a) and a uniform Pb film in (b).

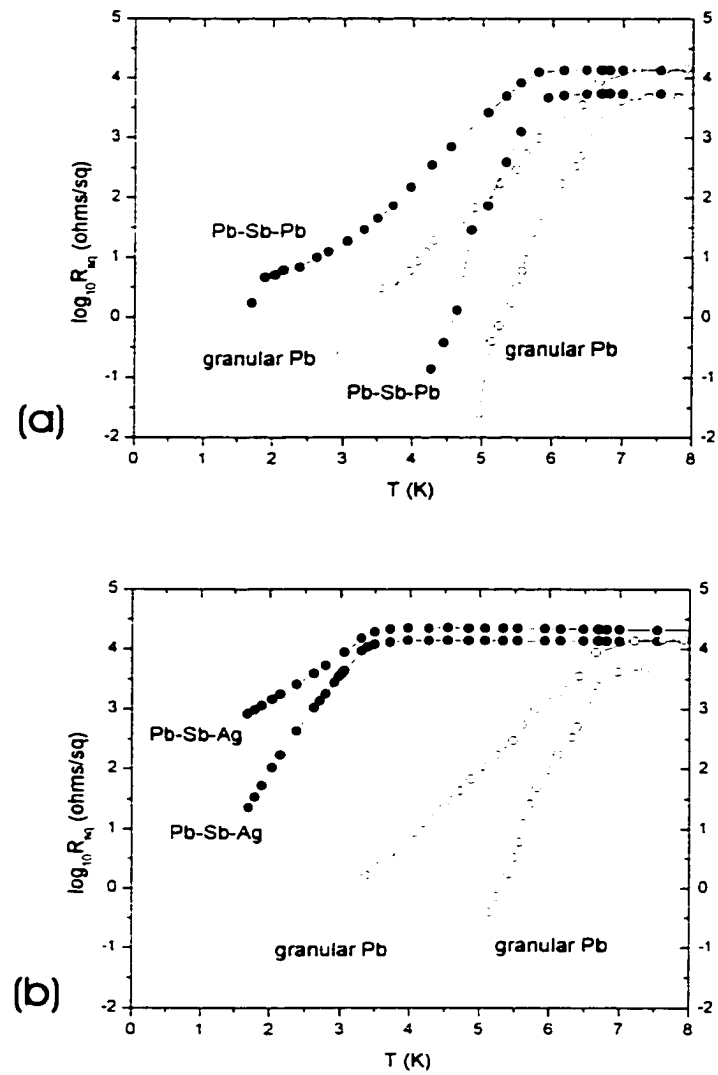

Figure 6.4: Comparison of Pb-Sb-Pb transport and Pb-Sb-Ag transport with granular Pb transport

Open circles refer to a quench condensed granular Pb film. Closed circles refer to a Pb-Sb-Pb film in a, and a Pb-Sb-Ag film in b. (a): Pb-Sb-Pb tail slope comparison with granular Pb (b):Pb-Sb-Ag tail slope comparison with granular Pb

then reduces the electrical barrier between the superconducting grains, and this improves the Josephson coupling.

To better investigate the similarities of the Pb-Sb-Pb film to granular Pb and uniform Pb, four plots are chosen at the S-I transition and plotted in figure 6.3. These four plots exhibit quasi-reintrant behavior in which the sheet resistance decreases below T_c, indicating weak overlap of superconducting wavefunctions, but then at some lower temperature, the sheet resistance increases, indicating decreased overlap and insulating behavior. There seems to be a competition between granular film and uniform film characteristics, and this extends the region of quasireintrance. At the normal state sheet resistance where a granular Pb film exhibits long resistive tail behavior in the weakly overlapping wavefunction region of the S-I transition, a Pb-Sb-Pb film is still competing between weak overlap and no overlap of the wavefunctions characteristic of quasireintrant transport. The trend toward overlapping wavefunctions is similar to that of a granular Pb film as seen in figure 6.3a, and the trend toward decreasing overlap of insulating behavior is reminiscent to that of a uniform Pb film as seen in figure 6.3b. The resistive slopes follow granular film transport at temperatures near a T_{MF} of 5.8 K, but as the temperature decreases past 3.8 K, the transport follows that of an insulating uniform film.

Exactly how the uniform film helps to couple Pb grains is very important. One can imagine a competing scheme between Josephson coupling of granular Pb and the uniform film tending toward an insulating state as the temperature decreases. The increasingly insulating transport of the uniform film, as the temperature decreases, reduces the Josephson coupling of the superconducting Pb grains. The quasiparticle conductance, provided by the uniform film, between the grains is rapidly decreasing as the temperature decreases.

Once the Pb-Sb-Pb film lies in the region of weakly overlapping wavefunctions of the S-I transition, the transport resembles the long resistive tails of granular Pb. As seen in figure 6.4a, two representative long resistive tails of Pb-Sb-Pb have the same slope as those of granular Pb. They share the same normal state sheet

resistance, and only the T_c of the Pb-Sb-Pb film is suppressed. In contrast, two representative long resistive tails of Pb-Sb-Ag share a common slope as those of pure granular Pb, but only at a normal state sheet resistance higher than the granular Pb film. This is interesting because at the same normal state sheet resistance, a Pb-Sb-Ag film has a sharper slope than that in a granular Pb film. Apparently the Ag of a Pb-Sb-Ag film has allowed phase fluctuations to be suppressed more at the same normal state sheet resistance than a granular Pb film.

The Pb-Sb-Ag film also exhibits some interesting transport behavior illustrated in figure 6.5: phase fluctuations are present in curve g, and are suppressed in h as seen by the sharp transition, and yet at a lower normal state sheet resistance, phase fluctuations reappear in i to give a resistive transition of some finite slope. With further deposition of Ag, the transition again sharpens up as seen in j. Thus the normal metal state sheet resistance alone does not appear to determine whether a slope will be gradual or sharp in a Pb-Sb-Ag film. It's possible that the coupling of the Cooper pairs and the amplitude of the order parameter are also important. It is known that a proximity effect between Pb and Ag will reduce the coupling of Cooper pairs. This was shown in chapter 5. The amplitude of the order parameter is important in determining the size of the supercurrent between Pb grains, and the amplitude is also a measure of the superfluid density. These three parameters could combine with each other to determine whether the resistive transition is sharp or gradual.

6.3 Proximity Effect

In the case of a Pb-Sb-Ag film, superconducting Pb grains lying under the Sb layer are a source of Cooper pairs for Ag grains that lie on top of the Sb layer. A uniform Ag film connects the Ag grains. As in the case of a thin Pb film, the thin Ag film may not be thick enough to support superconductivity, and may only exhibit insulating behavior. The superfluid density in a Ag grain is reduced from that in a Pb grain alone due to a proximity effect diluting Cooper pairs.

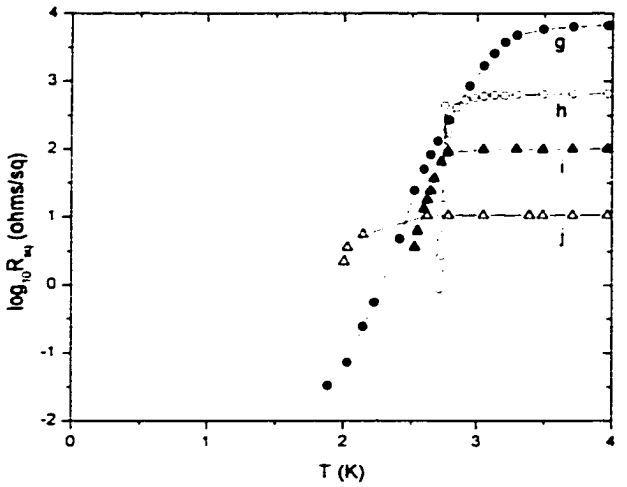

Figure 6.5: Transport of Pb-Sb-Ag film at low normal state sheet resistance.

In figure 6.6, the energy gap at T=0 and the corresponding film T_c is plotted for a Pb-Sb-Ag film. This is the same figure seen in chapter 5 for Pb/Ag films and the data are very similar except for one point at low energy gap near 0.2 meV. This discrepancy could be due to experimental limits since only a base temperature of 1.7 K could be measured for the tunneling data. When the tunneling data is plotted in figure 6.7a, however, this point seems more reasonable. The energy gap at T=0 was calculated using the BCS temperature dependence of $\Delta(T)$. The line is a guide to the eye, and points to a linear dependence of energy gap on the volume fraction of Ag. Notice the T_c calculated at half the normal state sheet resistance of a Pb-Sb-Ag film is not tending towards 0 as the volume fraction of Ag approaches 1. The T_c appears enhanced in figure 6.7b.

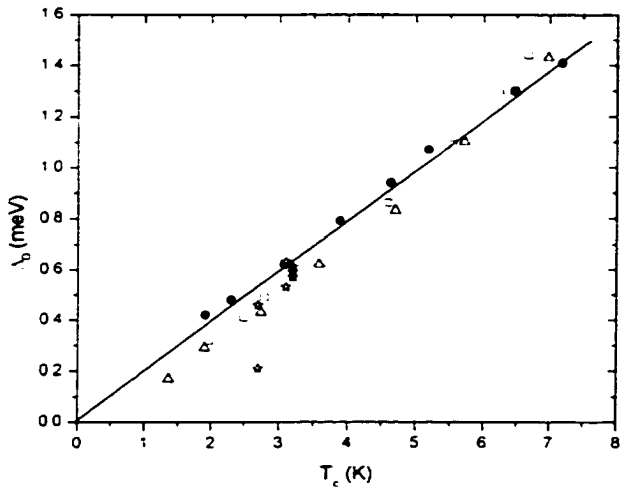

Figure 6.6: Energy gap at T=0 and corresponding film T_c

The open stars represent the Pb-Sb-Ag film. This is the same plot that appeared in chapter 5 except for the addition of Pb-Sb-Ag film values. The closed circles are for a uniform Pb film, and the open squares and open triangles are for a Pb/Ag film.

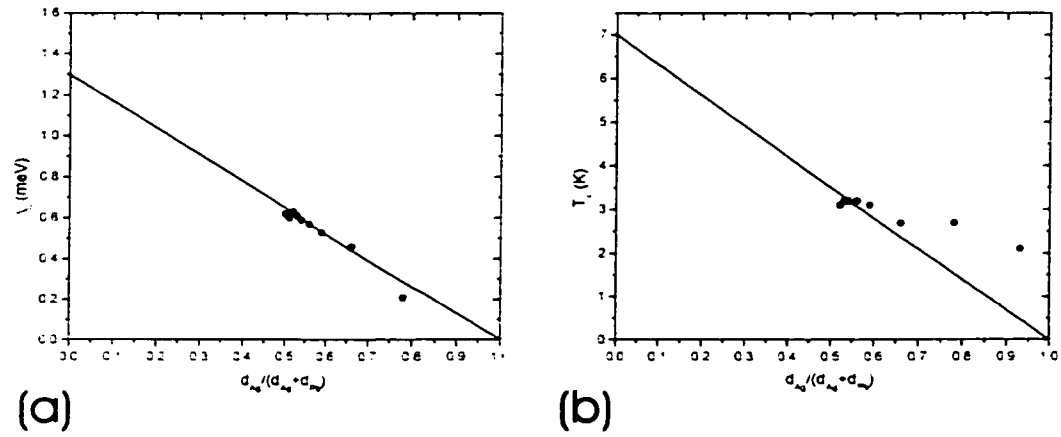

Figure 6.7: Energy gap and transition temperature of Pb-Sb-Ag film plotted versus fractional Ag thickness

Note that T_c does not appear to be suppressed to zero as the volume fraction of Ag approaches 1. The lines are guides for the eye.

6.4 Discussion

In chapter 4, we discussed granular Pb films coupled as a two-dimensional array of resistively shunted Josephson junctions. This same description can also work for the Pb-Sb-Pb/Ag films where the quasiparticle conduction method between superconducting grains is different. With Pb-Sb-Pb/Ag films, a uniform film on top of an Sb layer bridges (connects) superconducting grains also lying on top of Sb. The quasiparticle conduction of the junction is determined by the quasiparticle conduction of the uniform film, quasiparticle hopping, and quasiparticle tunneling.

This is very similar to the Emery-Kivelson model which stated that below the BCS mean field temperature T_{MF}, Cooper pairs exist, but they may not be phase coherent due to phase fluctuations. Phase fluctuations are intimately connected with the size of the Josephson binding energy, E_J. Phase fluctuations are likely to occur if the critical supercurrent I_c is not large enough to allow rapid transfer of Cooper pairs among different regions. This is due to the uncertainty relation between the number of pairs, N, and the phase, ϕ. Thus, the size of the critical

supercurrent and the Josephson binding energy is critical in determining whether phase fluctuations will prevent the phase coherence of all the Cooper pairs.

6.5 Conclusions

We find that the morphology of Pb-Sb-Pb films and Pb-Sb-Ag films strongly affects the superconducting behavior. The morphology at this point is only a proposal, and the true morphology is not known yet. But it seems the case that granular and uniform transport behavior has been combined. This was seen in the quasi-reintrant behavior seen over a larger range of normal state sheet resistance than in a pure granular Pb film. The Pb-Sb-Ag film pointed to some interesting behavior of varying resistive transition widths from sharp to wide where only a sharp transition was expected. More experiments would be interesting to probe the sheet resistance behavior to lower temperatures than 1.7 K.

Chapter 7

Conclusions

The experiments in this thesis have pointed toward the importance of phase fluctuations in disrupting long range superconductivity in a film. Granular Pb provides a nice system to explore phase fluctuations because it is composed of an array of locally superconducting grains which vary in Josephson coupling strength. A low T_c material is used with an agreed upon BCS theory of superconductivity. Analogies can then be made to high T_c materials where a theory of superconductivity is not agreed upon. Similarities are seen in the Emery-Kivelson theory of the film T_c phase diagram. Even though Cooper pairs exist and may be locally phase coherent, there is a finite resistance to the film. At first it is confusing that an array of Josephson junctions could be resistive since a supercurrent flows from one superconductor to the next in a Josephson junction. It is well known that a resistance results if the applied current is larger than the Josephson critical current, but how does a resistance result if the current is smaller than the critical current. One has to remember that these are very small grains with poor quasiparticle conduction between them. This and the density of Cooper pairs combine to determine the size of the Josephson binding energy, and in turn the size of the Josephson critical current. A simple washboard model of a Josephson junction illustrates that a thermal energy larger than the well depth of $E_J(T)$ can result in a 2π phase slip.

If a large enough uncertainty in particle number can be achieved between the regions, a well defined phase results. Long range superconductivity can then exist. This is due to the uncertainty relation between Cooper pair number, N, and phase, ϕ. $\Delta N \Delta\phi \sim \hbar$. The size of the critical supercurrent, I_c, determines how many Cooper pairs per unit time can be transferred between the regions. Anything that increases this transfer rate Q of Cooper pairs will result in a larger uncertainty in N, and thus larger certainty of phase. It turns out that Q depends on the product of quasiparticle conductance between regions and the energy gap, Δ. Increasing either will increase Q, and this increases the likelihood of phase locking.

This thesis explored many of the combination of parameters discussed above. Disorder in a uniform film affects the amplitude of the order parameter. Disorder in a granular film affects the phase of the order parameter. The proximity effect of Ag next to Pb affects the amplitude in Pb/Ag films and Pb-Sb-Ag films. Temperature was varied in all experiments, and this in turn varies $G_{q.p.}^{tot}$, $\xi(T)$, and $\Delta(T)$ which affect the amplitude and phase of the order parameter. The Emery-Kivelson theory was compared to granular Pb/Ag systems, and the parallels are amazing. Phase fluctuations are thus suggested to be very important in determining long range superconductivity in a material.

7.1 Future Experiments

It would be interesting to explore pair breaking in granular Pb films and study the effect on the S-I transition. Magnetic impurities can be deposited on top of a granular Pb film to induce pair breaking. One could then follow it by a Ag film to couple the grains. The initial grain size is then the same as a granular Pb film, but the Cooper pair density is reduced due to the magnetic impurities. The density is also reduced due to the proximity of Ag. The quasiparticle conduction may be the same as a granular Pb/Ag film, but the superconducting sheet resistance could be different.

Bibliography

[1] H. Onnes, Leiden Comm. **1206**, 1226 (1911).

[2] J. Bardeen, L. Cooper, and J. Schrieffer, Phys. Rev. **108**, 1175 (1957).

[3] L. Cooper, Phys. Rev. **104**, 1189 (1956).

[4] T. VanDuzer and C. Turner, *Principles of Superconductive Devices and Circuits* (Elsevier North Holland, Inc., New York, NY, 1981).

[5] V. Ginzburg and L. Landau, Ah. Eksperim. i. Teor. Fiz. **20**, 1064 (1950).

[6] M. Tinkham, *Introduction to Superconductivity* (McGraw-Hill, Inc., New York, 1996).

[7] D. Scalapino, *Tunneling Phenomena in Solids (ed. E. Burstein and S. Lundqvist)* (Plenum Press, New York, 1969).

[8] I. Giaever, Phys. Rev. Lett. **5**, 464 (1960).

[9] R. Dynes, J. Garno, G. Hertel, and T. Orlando, Phys. Rev. Lett. **53**, 2437 (1984).

[10] R. Dynes, V. Narayanamurti, and J. Garno, Phys. Rev. Lett. **41**, 1509 (1978).

[11] B. Josephson, Phys. Rev. Lett. **1**, 251 (1962).

[12] A. Barone and G. Paterno., *Physics and Applications of the Josephson Effect* (John Wiley and Sons, Inc., New York, 1982).

[13] P. Anderson, *Lectures on the Many-Body Problem, volume 2 (ed. E.R. Caianiello)* (Academic Press, New York, 1964).

[14] P. Anderson, *Quantum Fluids (ed. D.F. Brewer)* (North-Holland, Amsterdam, 1966).

[15] L. Cooper, Phys. Rev. Lett. **6**, 689 (1961).

[16] P. DeGennes, Reviews of Modern Physics **36**, 225 (1964).

[17] A. Herzog, Ph.D. thesis, University of California, San Diego, 1996.

[18] P. Lee and T. Ramakrishnan, Reviews of Modern Physics **57**, 287 (1985).

[19] M. Strongin, R. Thompson, and O. Kammerer, Phys. Rev. B **1**, 1078 (1970).

[20] H. Jaeger, D. Haviland, B. Orr, and A. Goldman, Phys. Rev. B **40**, 182 (1989).

[21] B. Orr, H. Jaeger, A. Goldman, and C. Kuper, Phys. Rev. Lett. **56**, 378 (1986).

[22] R. Dynes, J. Garno, and J. Rowell, Phys. Rev. Lett. **40**, 479 (1978).

[23] R. Barber, L. Merchant, A. L. Porta, and R. Dynes, Phys. Rev. B **49**, 3409 (1994).

[24] J. J.M. Valles, R. Dynes, and J. Garno, Phys. Rev. Lett. **69**, 3567 (1992).

[25] R. Richardson and E. Smith, *Experimental Techniques in Condensed Matter at Low Temperatures* (Addison-Wesley, Redwood City, CA, 1988).

[26] V. Emery and S. Kivelson, Nature **374**, 434 (1995).

[27] B. Muhlschlegel, Z. Phys. **155**, 313 (1959).

[28] H. Ibach and H. Lüth, *Solid State Physics: An Introduction to Theory and Experiment* (Springer-Verlag, Berlin, 1993).

[29] S. Woods, Ph.D. thesis, University of California, San Diego, 1998.